Available online at www.sciencedirect.com
SCIENCE DIRECT®
Bioorganic & Medicinal Chemistry 12 (2004) 5247–5268
Bioorganic & Medicinal Chemistry

Review

# Catalytic antibodies: hapten design strategies and screening methods

Yang Xu, Noboru Yamamoto and Kim D. Janda*

*The Scripps Research Institute, Department of Chemistry and The Skaggs Institute of Chemical Biology, 10550 North Torrey Pines Road, La Jolla, CA 92037, USA*

Received 25 February 2004; accepted 8 March 2004
Available online 11 September 2004

**Abstract**—Catalytic antibodies have emerged as powerful tools for the efficient and specific catalysis of a wide range of chemical transformations. Generating antibody catalysts that achieve enzymatic efficiency remains a challenging task, which has long been the source of great interest both in the design of more effective haptens for immunization and in the development of more direct and efficient screening methods for the selection of antibodies with desired catalytic capacities. In this review, we describe the development of different hapten design strategies, including a transition state analog (TSA) approach, 'bait-and-switch' catalysis, and reactive immunization. We also comment on recent developments in the screening process that allow for a more efficient identification of antibody catalysts.


## Contents



* Corresponding author. Tel.: +1 858 784 2516; fax: +1 858 784 2595; e-mail: kdjanda@scripps.edu

0968-0896/$ - see front matter © 2004 Elsevier Ltd. All rights reserved.
doi:10.1016/j.bmc.2004.03.077

## 1. Introduction

For over a decade, scientists have realized that the immune system is a rich source of intriguing and highly efficient catalysts for common organic synthesis reactions. These catalysts are antibodies that have been identified in the immune system using small molecules known as haptens. The hapten is rationally designed for a given targeted chemical reaction in the hope that the antibody it elicits will catalyze that reaction. Antibodies that perform the desired catalysis are then identified as catalytic antibodies, or 'abzymes'.

To date, catalytic antibodies have been shown to catalyze a vast array of different chemical processes, incorporating specificity, stereoselectivity, and even the ability to route a reaction through a disfavored chemical pathway. In fact, antibodies have now been uncovered for reactions for which there are no known natural or man-made enzymes.

There are many steps involved in realizing a successful catalytic antibody for a given chemical transformation. Of primary importance is the rational design of the hapten that will be used for immunization; one of the most widely applied strategies has been to employ antigens that are designed and prepared as transition-state analogs (TSAs) of the target reactions. Alternatively, haptens carrying a point charge have been employed in order to recruit a complementary charged amino acid in the antibody active site to perform catalysis, which has been termed the 'bait-and-switch' strategy. Recently, reactive immunization has been developed as another powerful strategy to provide a means for the selection of antibody catalysts in vivo on the basis of their reactivity.

Once the hapten has been designed and prepared, it is immunized as a conjugate with a carrier protein to provide sufficient immunogenicity to elicit an immune response. Any antibodies produced by the defense mechanism of the adaptive immune system that specifically recognize the hapten are then isolated for testing their catalytic activity towards the targeted chemical reaction. A variety of screening methods have been devised to facilitate fast and efficient selection of antibodies with desired catalytic activities from the products of an immune response.

This review will focus on recently discovered catalytic antibody generated against haptens designed by a variety of strategies (vide supra), as well as newly developed screening methodologies for the identification of antibody catalysts.

## 2. Hapten design strategies

### 2.1. Catalytic antibodies generated against transition-state analogs (TSAs)

As first described by Jencks, antibodies that are raised against an analog of the putative transition state of a given reaction may catalyze that reaction by lowering the activation energy by recognizing and binding to the transient transition state structure as it is formed during the reaction.[1] Based on this concept, haptens are designed to closely mimic the transition states and related high-energy intermediates with regards to fractional bond orders, lengths, and angles, as well as expanded valences, charge distribution, and geometry. The first successful examples of catalytic antibodies raised against haptens as TSAs were reported by Lerner and Schultz independently in 1986.[2,3] Since then, the TSA approach has been applied in a large number of studies in order to generate designer protein catalysts for many chemical transformations.

According to transition state theory,[4–6] the catalytic efficiency ($k_{cat}/k_{uncat}$) of a given enzymatic reaction can be deduced from the thermodynamic cycle (Scheme 1) under ideal conditions.[7,8] The following equations are established:

$$K_{TS}/k_{uncat} = K_s/k_{cat}$$

$$k_{cat}/k_{uncat} = K_s/K_{TS}$$

Here, the constant $K_{TS}$ is the dissociation constant for the antibody-transition-state complex, $k_{uncat}$ is the rate constant for the uncatalyzed reaction, $K_s$ is the dissociation constant for the antibody–substrate complex, and $k_{cat}$ is the rate constant for the reaction in the presence of antibodies. If the hapten used for immunization is a valid transition state analog of the target chemical process, the rate enhancement can be predicted from the ratio $K_S/K_{TSA}$ where $K_{TSA}$ represents the affinity of the antibody for the transition-state analog.

$$k_{cat}/k_{uncat} = K_s/K_{TS} = K_S/K_{TSA}$$

Haptens are often designed to mimic a high-energy intermediate en route to forming the desired product; such haptens are referred to as transition state analogs. According to transition state theory, a transition state is a short-lived theoretical species that is believed to occur at the energetic peak in a reaction pathway, being transient with no finite lifetime. Ideally, it is this structure that a hapten should mimic. In practice, however, the closest structure that is isolable and practical to work with, a 'working' transition state analog, is what is typically used. Finally, manipulating bond lengths and charge distributions may also lead to mimics of the transition state, but obviously not exact replicas.

**2.1.1. Antibody-catalyzed acyl transfer reactions.** Ester and amide hydrolysis are known to involve high-energy

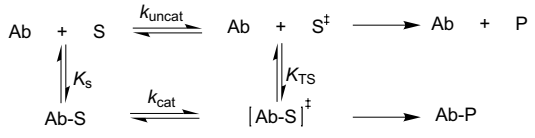


**Scheme 1.**

tetrahedral intermediates that decompose into the corresponding carboxylic acid and alcohol or amine, respectively. This high-energy intermediate and corresponding transition state can be mimicked by phosphonates, phosphonamidates, arsonates, and sulfonates, all of which contain the key tetrahedral structural motif and are often employed in the design of TSA haptens for immunization.

Catalytic antibodies as designer proteases and esterases have been reviewed by Tanaka in 2002.[6] Most of these antibodies fulfill the relationship $k_{cat}/k_{uncat} = K_S/K_{TSA}$ The mechanism of antibody-catalyzed reactions are in general validated by showing that the transition-state analog used to elicit the antibody inhibits catalysis in a competitive fashion and, furthermore, binds with a higher affinity than the corresponding substrate.

Amide hydrolysis remains a difficult task due to the fact that an amine is in general a very poor leaving group. In the design of amidase antibodies, phosphinates, and phosphonamidates—which are ionized at physiological pH—came to the fore as the preferred haptens. However, few amide-cleaving antibodies have been obtained. One notable example is antibody 43C9, which not only catalyzes the hydrolysis of aromatic amides and esters, but also shows an exceptional rate acceleration ($2.5 \times 10^5$ over background reaction).[9–11] Antibody 43C9 was induced with a tetrahedral transition state mimic, phosphonamidate **1** (Scheme 2). The unusually high rate enhancement of this antibody suggested a more intricate catalytic mechanism than mere proximity of reactive groups accompanied by modest transition state

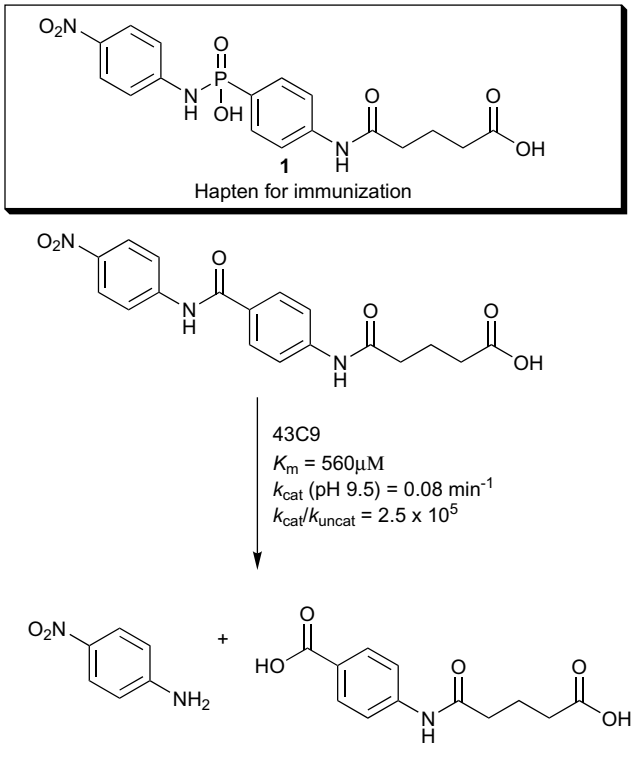


**Scheme 2.** Antibody 43C9 was elicited by hapten **1**. It catalyzes the hydrolytic reaction shown.

stabilization. In 1994, Roberts et al. constructed a computational model to investigate the structural basis for the catalytic activity of antibody 43C9.[12,13] This model implicated $Arg^{196}$ in stabilizing the transition state and $His^{191}$ as a neutral nitrogen nucleophile. In order to investigate the precise catalytic mechanism of 43C9, crystallographic structures of the 43C9 scFv (single-chain variable fragment), both bound and unbound to the esterolytic product *p*-nitrophenol, have been determined.[14] These crystallographic data fully support the computational model, indicating that transition-state stabilization through an extensive hydrogen-bonding network is important in catalysis. However, 43C9 is unique in having a nucleophile well-positioned at the binding pocket, which may be the key for amide hydrolysis. Yet, the active site of 43C9 is similar to those of other esterase antibodies, such as CNJ206, 48G7, and particularly 17E8.[14] Recently, Chong et al. carried out quantum mechanical calculations, molecular dynamics simulations, and free energy calculations to assess the mechanism involving direct hydroxide attack for antibody 43C9, with the results supporting this mechanism.[15] Furthermore, they suggested that this direct hydroxide attack mechanism is plausible for other antiphosphonate antibodies tailored for the hydrolysis of (*p*-nitro)phenyl esters.

Amidase antibody 312D6 was obtained against the sulfonamide hapten **2** (Scheme 3), which mimics the tetrahedral intermediate as well as the related transition state of a distorted amide hydrolysis.[16] It appeared that even though sulfonamides adequately reproduce the geometry and conformation of tetrahedral intermediates for the base-catalyzed hydrolysis of amides, they do not provide the same charge distribution. It was speculated, however, that for highly reactive amides, a neutral hydrolysis pathway corresponding to the uncatalyzed addition of water might operate at near-neutral pH. Therefore, it is reasonable to assume that a sulfonamide is a better mimic for the neutral species involved along the hydrolytic pathway. By using the sulfonamide as a hapten, it is also anticipated that antibodies generated upon binding the substrates will force them to adopt a twisted conformation in which the highly distorted amide bond would be more susceptible towards hydrolysis. Hapten **2** was used for immunization as a KLH (keyhole limpet hemocyanin) conjugate, and hapten **3** was used for ELISA (enzyme linked immunosorbent assay) screening as a BSA (bovine serum albumin) conjugate. Two antibodies showed hydrolytic activity above background levels, and 312D6 proved to be the most active catalyst.

**2.1.2. Antibody-catalyzed cationic cyclization.** Antibody HA519A4 catalyzes the tandem cationic cyclization of a polyene substrate (Scheme 4).[17] To date, this antibody is the only one that has been analyzed at atomic resolution. X-ray crystallographic data of the Fab fragment of HA519A4 co-crystallized with eliciting hapten **4**, designed as a TSA, suggested that the hapten is deeply buried within a hydrophobic pocket.[18] The antibody combining site provides a highly complementary fit as well as multiple aromatic residues. Therefore, it appears

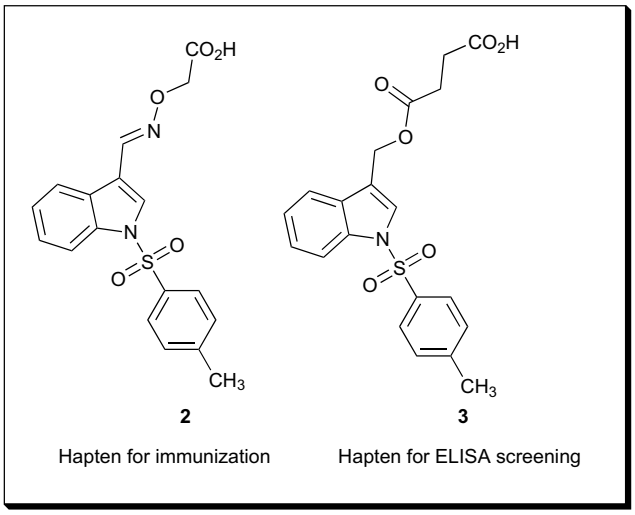


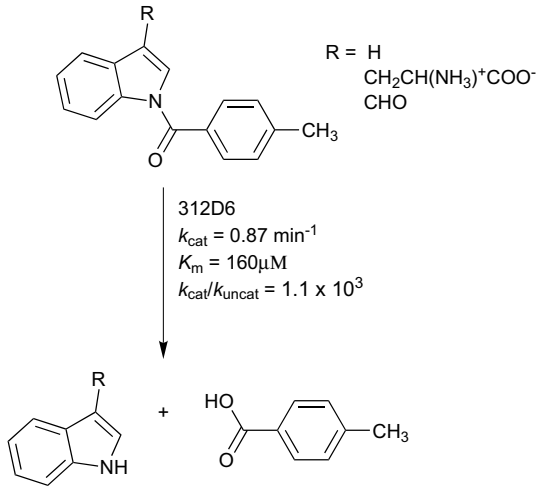


**Scheme 3.** Antibody 312D6 was elicited by hapten **2**. It catalyzes the hydrolytic reaction shown.

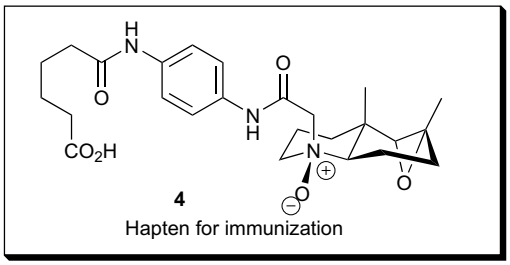


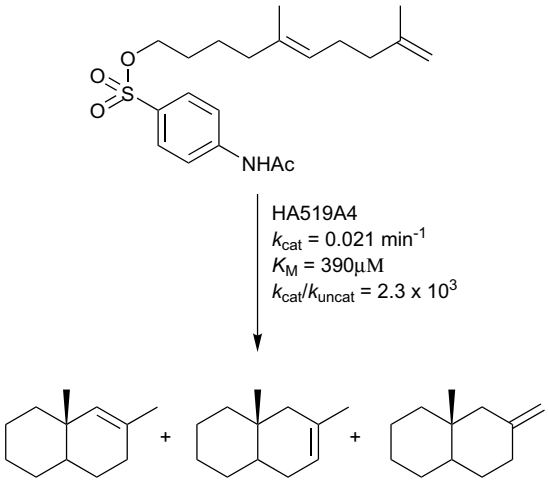


**Scheme 4.** Antibody HA519A4 was elicited by hapten **4**. It catalyzes the cationic cyclization reaction shown.

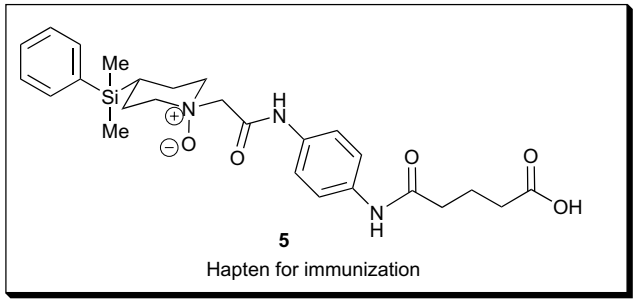


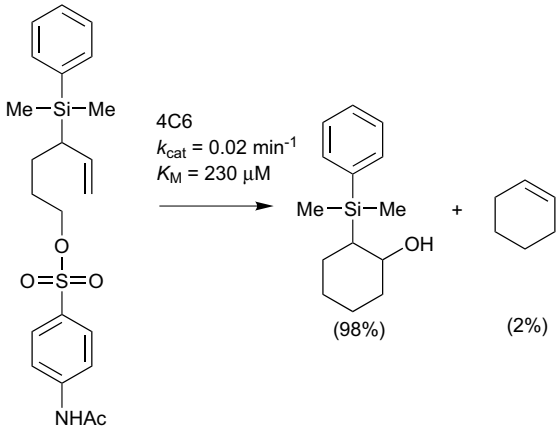


**Scheme 5.** Antibody 4C6 was elicited by hapten **5**. It catalyzes the cationic cyclization reaction shown.

that upon binding the polyene, the active site of the antibody forces it into the productive chair-chair conformation.

Recently published crystal structures of antibody 4C6, an antibody that catalyzes another cationic cyclization reaction (Scheme 5),[19] revealed that this antibody has exquisite shape complementarity to its eliciting hapten **5**.[20] The active site contains multiple aromatic residues, which shield the high-energy intermediate from solvent and stabilize the carbocation intermediates through cation–π interactions.

**2.1.3. Antibody-catalyzed disfavored ring closure.** One dramatic feature of antibody catalysts is their ability to reroute reaction pathways, thereby achieving disfavored chemical transformations instead of favored low-energy chemical processes. An archetypal example is the antibody-catalyzed disfavored 6-*endo*-intramolecular cyclization reaction of *trans*-epoxyalcohol (Scheme 6). Due to the significant stereoelectronic constraints predicted by Baldwin's rules,[21,22] the uncatalyzed cyclization of *trans*-epoxyalcohol proceeds via the 6-*exo* pathway, affording tetrahydrofuran. Hapten **6a** was

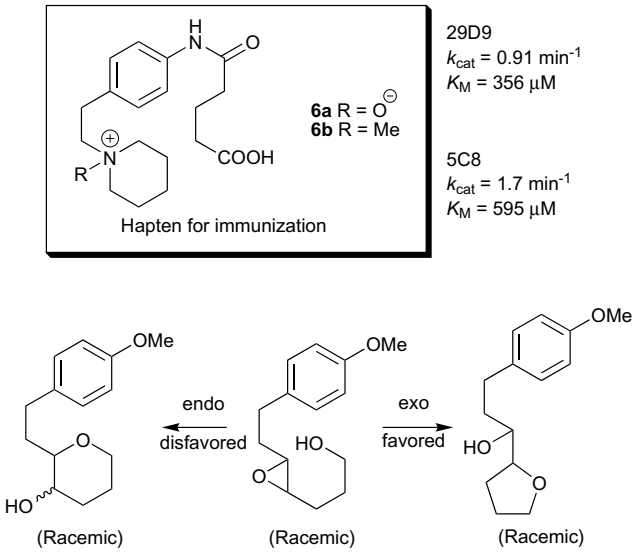


**Scheme 6.** Antibody 29D9 and 5C8 were elicited by hapten **6a** and **6b**, respectively. They both catalyzes the disfavored intramolecular cyclization reaction shown.

designed to mimic the stereoelectronic features of the disfavored 6-*endo*-transition state, where the N-oxide functional moiety mimics the electronic polarization of the epoxide in the transition state. The piperidinium ring provides the required pyran chair conformation of the disfavored product.[23] Antibody 26D9 was obtained, which was able to reroute the reaction process yielding tetrahydropyran as the only product. As an alternative, N-methyl ammonium **6b** was used in the immunization. Antibody 5C8 was uncovered as a catalyst for the regio- and enantio-selective disfavored *endo*-ring opening of the substrate. The X-ray structures of two complexes of Fab 5C8 with the eliciting hapten and with an inhibitor were recently published.[24] The active site of the antibody contains a putative catalytic diad, consisting of $Asp^{H95}$ and $His^{L89}$ that perform general acid/base catalysis.

**2.1.4. Antibody-catalyzed Diels–Alder reaction.** The Diels–Alder reaction is of particular interest for chemists not only because it is a rare reaction in nature, but also because of the fact that it proceeds via an entropically disfavored, highly organized transition state.[25] To date, a number of antibody Diels–Alderases have been reported.

Antibody 1E9 was elicited against the *endo*-hexachloronorbornene derivative **7**, which is a stable analog of the high-energy transition state for the cycloaddition between tetrachlorothiophene dioxide and N-ethylmaleimide (Scheme 7).[26] Since this reaction liberates $SO_2$ spontaneously and oxidizes to form the aromatic product, which is structurally dissimilar to the hapten, no product inhibition was detected. From the X-ray crystallographic data of Fab fragment of 1E9, it was revealed that the antibody binding pocket is preorganized to provide significant shape complementarity with the hapten through Van der Waals contacts, π-stacking with the maleimide functional moiety, and a hydrogen

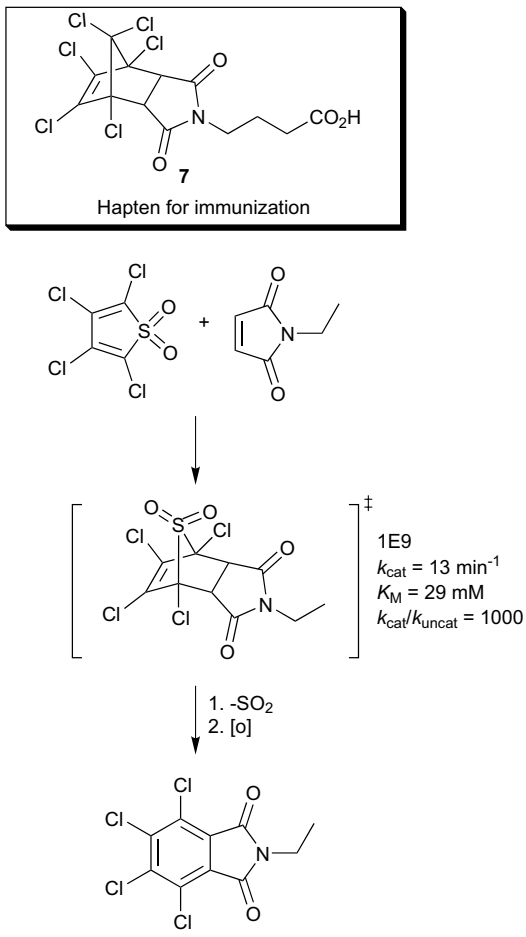


**Scheme 7.** Antibody 1E9 was elicited by hapten **7**. It catalyzes the Diels–Alder reaction shown.

bond with $Asn^{H35}$.[27] In a recent study, Kim et al. surveyed Diels–Alder reactions catalyzed by noncovalent binding to synthetic, protein, and nucleic acid hosts.[28] Antibody 1E9 was revealed as the most effective catalyst of the noncovalent catalyst systems studied. This extraordinary catalytic capability has been explained by theoretical calculations and results indicated that 1E9 has a high degree of shape complementarity, consistent with the X-ray crystallographic data.[27]

Antibody 39-A11 was raised against bicyclo[2.2.2]octane hapten **8**, which was designed as a mimic of the proposed boat-like transition state of the 4π + 2π cycloaddition between diene **9** and dienophile **10** (Scheme 8).[29] Product inhibition is circumvented by the structural disparity between the product cycloadduct and the pseudoboat form of the hapten employed for immunization. The X-ray crystallographic data of the Fab fragment of 39-A11[30] as a complex with the hapten has been reported.[31] It was revealed that the antibody binds the diene and the dienophile in a reactive conformation and presumably reduces translational and rotational degrees of freedom. The binding of enantiomeric haptens by antibody 39A11 was studied theoretically by Zhang et al. in an investigation of mechanism of stereoselective hapten binding by this Diels–Alderase antibody using

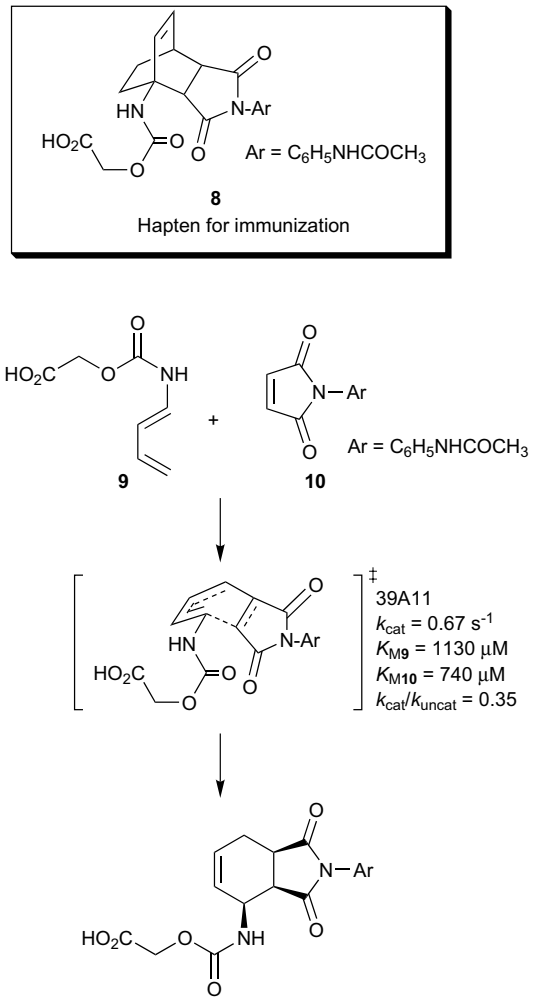


**Scheme 8.** Antibody 39A11 was elicited by hapten **8**. It catalyzes the Diels–Alder reaction shown.

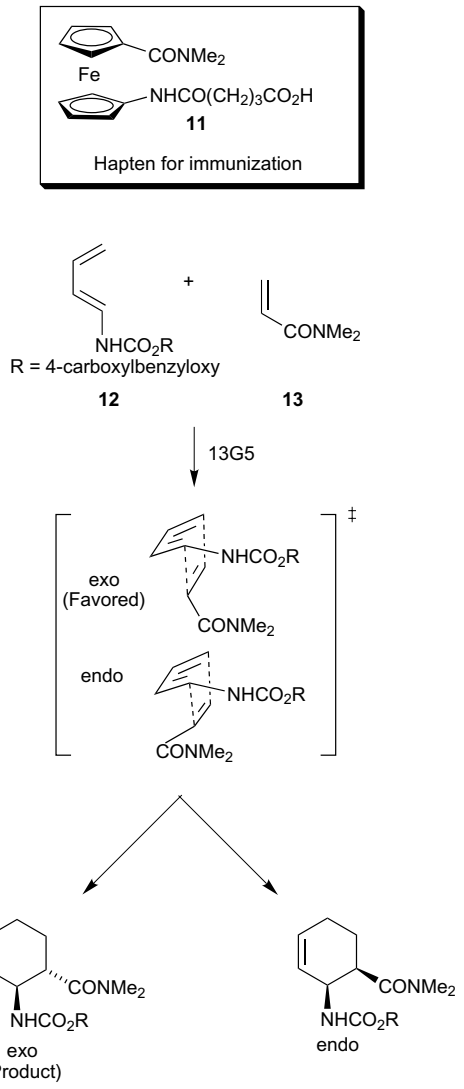


**Scheme 9.** Antibody 13G5 was elicited by hapten **11**. It catalyzes the *exo*-cycloaddition shown.

docking simulations and quantum mechanical models.[32] Based on these data, they predicted that the stereoselectivity of 39A11 was accomplished by two strategically positioned hydrogen bonds and π-stacking of the maleimide with a tryptophan at the antibody binding site. This unique arrangement allows reorganization of one enantiomeric transition state (Scheme 8).

As a new approach to produce Diels–Alderase antibodies that could catalyze the formation of either the *exo*- or *endo*-cycloadducts, Janda and co-workers have employed a ferrocenyl hapten **11**.[33] This hapten is highly flexible with the cyclopentadienyl rings able to rotate freely in solution. Antibody 13G5, raised against **11**, is able to catalyze the disfavored *exo*-cycloaddition reaction between **12** and **13** in high regio-, diastereo-, and enantio-selectivity (Scheme 9). The crystal structure of the 13G5 Fab complexed to an attenuated form of hapten was determined.[34] It was shown that the ferrocene moiety is completely buried in the antibody combining site, and the ferrocene ring rotation is restricted by the steric restraints imposed by specific hydrogen-bonding interactions with the antibody binding pocket.

Cannizzaro et al. synthesized the enantiomerically pure Diels–Alder adduct obtained by antibody catalysis with 13G5 and other monoclonal antibodies elicited during the same immunization process.[35] Based on this information, they established enantioselectivity of these antibodies and the effects of different catalytic residue arrangements on the transition states were modeled quantum mechanically. Results provided an explanation of the origin of the observed enantioselectivity of 13G5. It was depicted in their study that the hapten molecule **11** used for screening antibodies for binding to TS analogues resembles the Van der Waals complex between the reactants more closely than the transition state; this selection process yields binders that preferentially recognize the rotamer of the hapten that mimics the (R, R) TS analogues.

The first example of an antibody-catalyzed aza Diels–Alder reaction was reported by Shi et al. recently.[36] Hapten **14** was designed as a TSA (Scheme 10), and a polyclonal antibody Aza-BSA-3 was discovered to catalyze the desired aza Diels–Alder reaction.

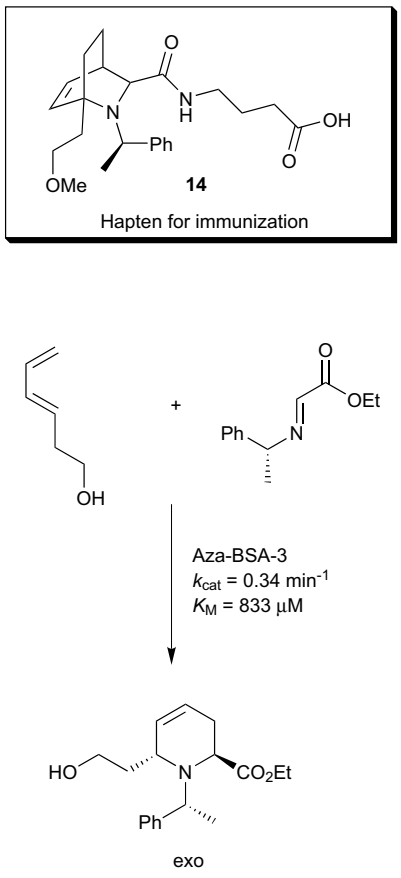


**Scheme 10.** Antibody aza-BSA-3 was elicited by hapten **14**. It catalyzes the aza Diels–Alder reaction shown.

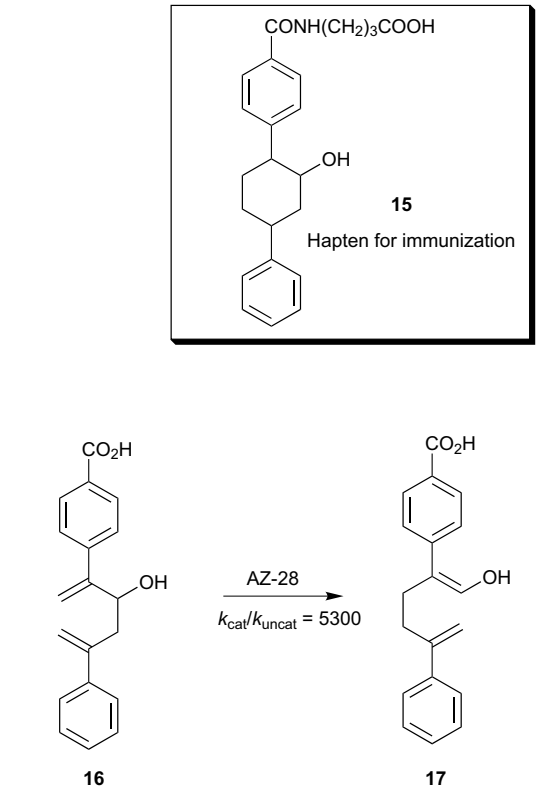


**Scheme 11.** Antibody AZ-28 was elicited by hapten **15**. It catalyzes the oxy-Cope rearrangement shown.

**2.1.5. Antibody-catalyzed oxy-Cope rearrangement.** The oxy-Cope rearrangement is a [3,3] sigmatropic rearrangement, which occurs via a highly organized chair-like transition state.[37,38] An antibody catalyst for such a reaction must be able to bind the substrate and orient the ground state into this productive chair-like conformation. Antibody AZ-28 was raised against the chair-like transition state analog **15**, which catalyzes the oxy-Cope rearrangement of **16** to produce **17** (Scheme 11).[39] Product inhibition and chemical modification of the antibody are prevented by in situ generation of the oxime. Surprisingly, the germline precursor of AZ-28, which has a much lower affinity toward the eliciting hapten, accelerated the reaction 164,000-fold over the uncatalyzed background reaction. In order to study the structural basis for binding and catalysis, the X-ray crystal structures of AZ-28, apo-form and complexed with the eliciting hapten have been determined.[40] In the antibody–hapten complex, the TSA is fixed in a catalytically unfavorable conformation by a combination of Van der Waals and hydrogen-bonding interactions. In contrast, the active site of the germline precusor of AZ-28 appears to have a much higher degree of flexibility; specifically, the CDRH3 moves 4.9 Å outwards from the active site upon binding the eliciting hapten. It was initially proposed that this conformational flexibility in the germline antibody allows dynamic changes that lead to enhanced orbital overlap and increased rate acceleration. This mechanistic explanation was further substantiated by a molecular dynamics simulation study by Asada et al.[41]

**2.1.6. Antibody-catalyzed hydride transfer.** Alcohol dehydrogenases catalyze the oxidation of alcohols to aldehydes and simultaneously reduce the nicotinamide derivatives $NAD^+$ and $NADP^+$ to the corresponding 1,4-dihydronicotinamides.[42,43] Compounds **18** and **19** were designed and prepared as stable TSAs for the hydride transfer process between **20** and an aliphatic aldehyde to distinguish specific antibody catalysis from contaminant dehydrogenases (Scheme 12).[43] These haptens incorporated a rigid [3.2.2] bicyclic structure that contain a 3-piperidone oxime, wherein the oxime motif mimics the carboxamide group in nicotinamide. The piperidone is held in the boat conformation corresponding to the transition state by a three-atom lactam bridge. The aldehyde carbon in the transition state was mimicked by a methylene group in **18**, while in hapten **19**, it is mimicked by a sulfonyl group. The production of monoclonal antibodies against these novel haptens and their kinetic characterization has not been reported to date.

**2.1.7. Issues with TSA-based approaches.** In the search for antibody catalysts using TSAs as eliciting compounds, a significant fraction of hapten binders failed to catalyze the target reactions. This is not difficult to understand since during an immune response, hapten affinity rather than catalytic activity drives maturation of the immune response. Therefore, somatic mutations

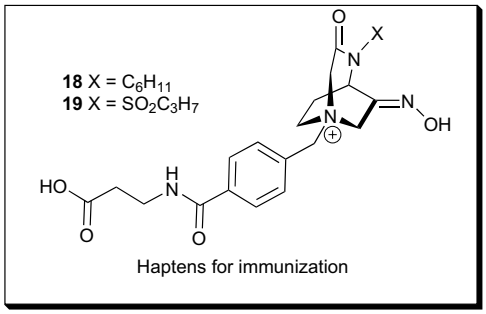


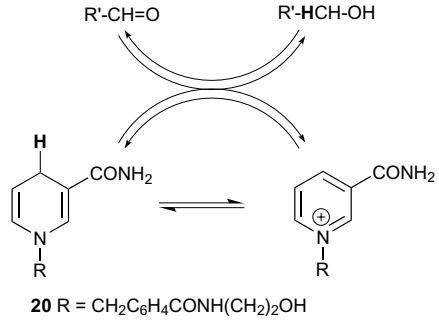


**Scheme 12.** Haten **18** and **19** were designed for the targeted hydride transfer reaction.

can raise antibodies that favor tighter hapten binding but are deleterious for catalysis.

It appeared early on that antibody catalysts are limited in their capability to accelerate chemical reactions as efficiently as natural enzymes in terms of efficiency $((k_{cat}/K_M)/K_{uncat}$ or $1/K_{TS})$.[8,44,45] Published $K_{cat}/K_M$ values of catalytic antibodies range from $10^2$ to $10^4\,M^{-1}S^{-1}$, while those of natural enzymes range from $10^6$ to $10^8\,M^{-1}S^{-1}$.

It is crucial that antibody catalysts raised against TSAs have to release the product to be considered efficient, but in a number of cases, the products of the reaction bear a high degree of structural similarity to the TSAs used in immunization. Slow release of product—product inhibition at the antibody combining site—has been considered as a major contributing factor for the low efficacy of hydrolytic antibodies.[46–48]

One possibility for the poor performance of some transition state analog-based antibody catalysts may be an inability to design a stable organic compound that could reproduce the fractional bond orders, extended bond lengths, expanded valences, distorted bond angles, and charge distributions in the fleeting structure of a transition state. Considering that transition states can share recognition elements with ground state molecules, it seems obvious that the TSAs would never achieve geometries and charge distributions of transition states precisely.[49] For example, when using a phosphonate motif[50,51] to design haptens to elicit hydrolytic antibodies, there are obvious discrepancies in reproducing the exact bond length and charge distribution compared to the real transition state structure evolved during the reaction process.[52] Recently, Tantillo and Houk examined the properties of transition states and the high-energy intermediates involved in the hydrolysis of phenyl and *p*-nitrophenyl acetate and compared them with haptens designed according to the TSA strategy.[53] The results suggested that even though aryl phosphonates mimic some of the geometric features of the transition states and intermediates, they less faithfully mimic the asymmetry and electrostatic properties of these stationary states involved in the reaction process. In particular, the haptens seem more similar to the elimination transition state and tetrahedral intermediate in terms of molecular size, bond lengths, and bond angles; they bear little resemblance to the addition transition state or the reactant or product complexes.

For the majority of catalytic antibodies, recognition of antigens is mediated through interactions including Van der Waals interactions, hydrogen bonding, and other electrostatic and hydrophobic forces, which is very similar to enzyme-substrate binding. In a recent review, Houk et al. surveyed the binding affinities of host–guest, protein–ligand, and protein–TS complexes.[54] In the case of catalytic antibodies, comparison of kinetic data[55] revealed that the transition states for typical antibody-catalyzed reactions are bound $10^3$ times more strongly than the substrates. Dissociation constants of catalytic antibodies and transitions states of the reactions they catalyze fall in the $10^{-6.6}$–$10^{-8.6}$ range, while the dissociation constants of catalytic antibodies and substrates fall in the range of $10^{-2.4}$–$10^{-4.6}\,M$. This selectivity in guest recognition provided the basis for tailoring antibodies as catalysts. However, the strongest binding involves enzymes and transition states of the reactions they catalyze; typical enzyme–TS complexes have dissociation constants in the picomolar ($10^{-12}\,M$) to zeptomolar ($10^{-14}\,M$) range. This massive binding constant of enzymes are attributed to billions of years of evolution, which incorporated strong electrostatic interactions as well as metal cofactors, acid-base chemistry, and most importantly covalent interactions between the enzyme and transition state.[8]

Of critical importance for the catalytic proficiency of natural enzymes is that their catalytic machinery and bound substrates are often buried. This feature sequesters the reactive functionalities, which mediate chemical transformations from the solvent.[8,56] In antibody catalysis, however, the moieties of the bound haptens that mimic the transition state are often positioned near the entrance of the antibody-combining site. This disparity in the overall architecture of natural enzymes and catalytic antibodies is undoubtedly a factor in the lower catalytic proficiency of the latter. Houk's review discussed the relationship between average binding constants and the average surface areas buried upon binding. Based on the thermodynamic data available for protein-substrate complexes, he pointed out a clear trend between the buried areas of the guests and binding affinities- 67′ of accessible surface area of guest is buried for $1\,kcal\,mol^{-1}$ binding energy.[54] It is also notable that the manner in which haptens are attached to carrier proteins

gives rise to significant differences in certain cases.[57] Haptens designed with aromatic moieties between the linkage to the immunogenic carrier protein and the TSA motif often yield better antibody recognition.

Recently, Hilvert pointed out that on both micro and macro levels, mechanistic improvement arise as a function of time.[58] The differences in time scales for the evolution of natural enzymes and antibodies—millions of years versus weeks or months—also appear to be an explanation of the low efficiency of antibody catalysts. He also highlighted that the unique immunoglobulin fold has not been adopted by nature as one of the common scaffolds on which to build enzyme catalytic machinery. Therefore, antibody structure itself places limitations on the kind of reactions amenable to catalysis.

### 2.2. 'Bait-and-switch' strategy

Small compounds that carry positive or negative charges could be used for the induction of complementary charged amino acid residues in the antibody-binding site. Based on this fact, a new approach for hapten design has been developed to expand the scope of antibody catalysis. This strategy involves the placement of a point charge on the hapten in close proximity to, or in direct substitution for, a chemical functional group that is expected to transform the corresponding substrate. The haptenic charge is expected to induce a complementary charge at the active site. The charged amino acid residues thereby recruited contribute to catalysis as general-acid/base or nucleophilic catalysts. Since the haptens designed according to this strategy serve as 'bait' for eliciting catalytic functions during the immunization process, which is then 'switched' for the substrate, the strategy has been named 'bait-and-switch'.[59,60]

The hydrolysis of phosphodiester bonds, which are often found in DNA and RNA, is a reaction of significant importance in living systems. Antibody MATT.F-1, which was raised against a quaternary ammonium hapten, is the most proficient antibody catalyst generated for the phosphodiester hydrolysis reaction (Scheme 13).[60] Hapten **21** was designed according to the bait-and-switch paradigm with the sole purpose of incorporating a general base in an antibody binding site proximal to the 2′ hydroxy of substrate **22** to facilitate nucleophilic attack of this hydroxyl group on the adjacent phosphoryl center. Note that in this case, the transition state mimicry is sacrificed and replaced by a point charge. MATT.F-1 has a catalytic proficiency ($(k_{cat}/K_m)/k_{uncat}$) of $1.6\times10^7\,M^{-1}$, which is higher than that reported for 2G12, elicited to the transition state analog hapten **23**. Perhaps most impressive, however, is that the proficiency of MATT.F-1 is only three orders of magnitude lower than that of the naturally occurring enzyme RNAseA for the same substrate.

Antibody HA8-25A10 was obtained from immunization with aza-steroid **24**, which bears an aminoxide oxygen at the beta position.[61] Antibody HA8-25A10 is capable of catalyzing the cationic cyclization of 2,3-epoxy-squalene derivatives (Scheme 14). The N-oxide moiety in hapten **24** was incorporated in order to elicit an acidic residue at the desired location within the active site. This hapten was anticipated to act both as a bait-and-switch hapten and a transition-state analog. This antibody initiated the cyclization through epoxide opening, but the propagation to the desired multicyclic ring system was not observed.

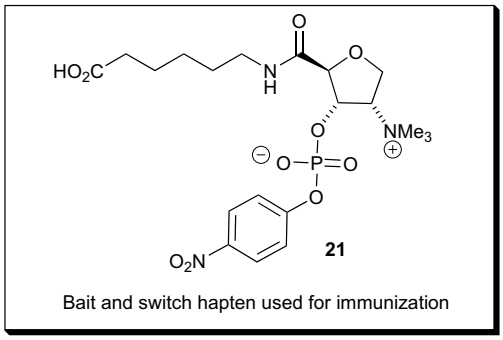


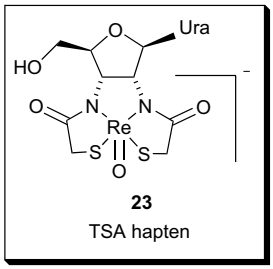


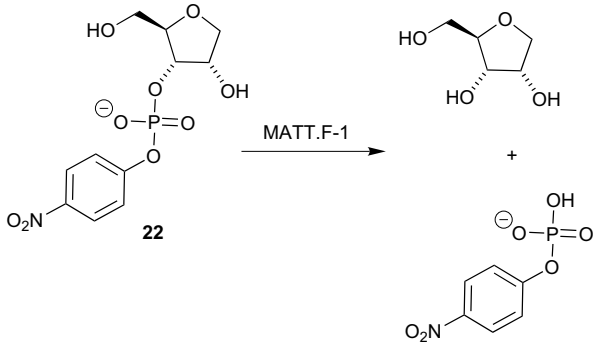


**Scheme 13.** Antibody MATT.F-1 was elicited by the bait and switch hapten **21**. It catalyzes the hydrolysis of phosphodiester bond shown.

4B2 is an antibody that catalyzes the allylic isomerization of β,γ-unsaturated ketones (Scheme 15).[62] The hapten, a substituted amidine **25**, is expected to elicit, by charge complementarity, an acidic residue (Asp or Glu) in the combining site. The presence of Asp and Glu in the complementarity-determining region (CDR) was later confirmed by cloning and sequencing the light and heavy chains of the 4B2. With this antibody catalysis scheme the α-proton exchanges on the same substrate, suggesting that a dienol intermediate is involved in the reaction process.

### 2.3. Reactive immunization

Many antibody catalysts have been generated by immunization with antigens that mimic the geometric and/or

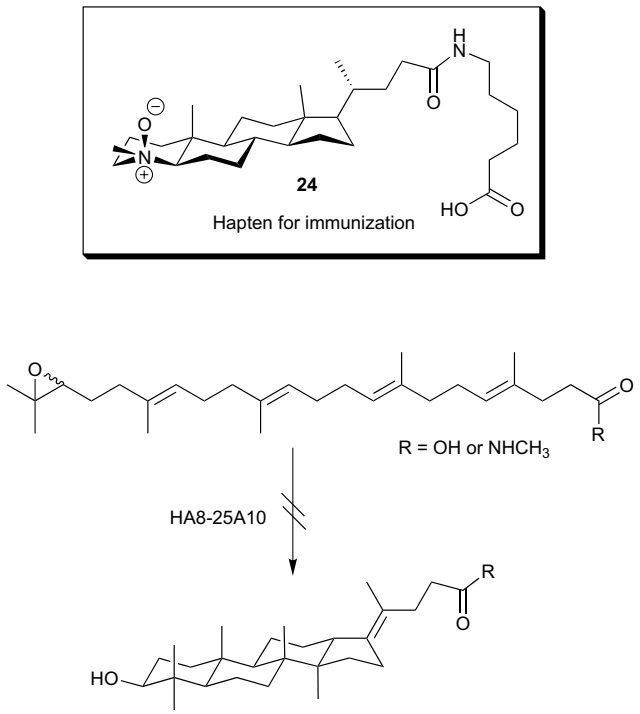


**Scheme 14.** Haten **24** was designed for the targeted cyclization reaction shown.

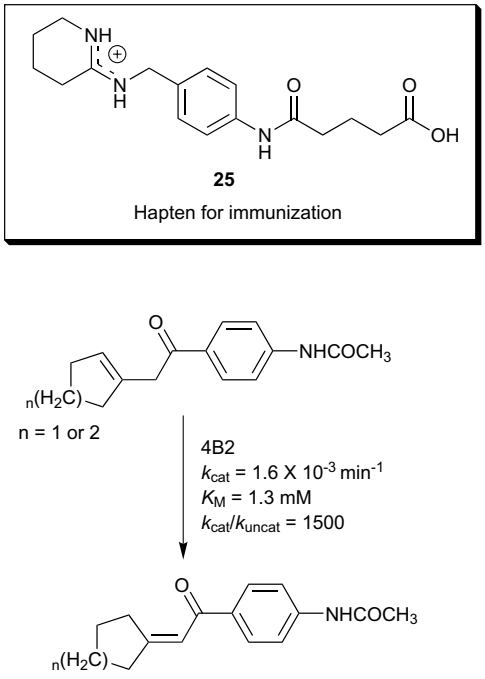


**Scheme 15.** Antibody 4B2 was elicited by hapten **25**. It catalyzes the allylic isomerization of β,γ-unsaturated ketone shown.

electronic features of a reaction's transition state. Both the TSA and bait-and-switch strategies employed rely for the most part on chemically inert antigens. A new hapten design strategy—reactive immunization—provides a chance for catalytic antibodies to approach the catalytic efficiency of natural enzymes through the use of reactive immunogens.[63]

In 1995 Janda, Lerner and co-workers pioneered the use of a highly reactive antigen that undergoes a chemical reaction in the antibody-combining site during immunization.[64] In the first attempt to examine this strategy, they designed an organophosphorus diester hapten **26** as the primary reactive immunogen for immunization. This hapten can be either hydrolyzed at physiological pH or trapped by a nucleophile at the B-cell level of the immune response affording the monoester **27**, an analog of the transition state (Scheme 16). Nineteen mAbs (monoclonal antibodies) were isolated, eleven of which were able to catalyze the target acyl-transfer reaction, hydrolysis of phosphonate diester **28** to generate the monoester **29**, in a one-turnover inactivation of the antibody (Scheme 17). Amongst these eleven catalytic antibodies, SPO49H4 demonstrated the best catalytic activity; it effectively catalyze the hydrolysis of the activated ester **30** to yield carboxylic acid **31** with a $k_{cat}$ of $31\,min^{-1}$ and a rate acceleration ($k_{cat}/k_{uncat}$) of 6700 at pH 8.0.

The first direct comparison between reactive immunization and transition state analog hapten manifolds for catalytic antibody production was demonstrated by comparing esterase antibodies elicited against a TSA, phosphonate monoester **36**, with the ones raised by a reactive immunogen, phosphonate diester **35**.[65,66] Hapten **35** was initially design for the purpose of resolving a racemic mixture of naproxen esters. Antibody 15G2 elicited to hapten **35** catalyzed the homochiral production of the anti-inflammatory agent Naproxen, *rac*-**33**, from **32**, incorporating stereoselective activity and disposition, the *S*-(+)-enantiomer **33a** of naproxen being formed 28 more times than the *R*-(−)-enantiomer **33b** (Scheme 18). This antibody catalyzed the hydrolysis of *S*-(+)-**32a** and gave *S*-(+)-**33a** with a $k_{cat} = 28\,min^{-1}$, $K_m = 300\,\mu M$ at pH 8.0, and $k_{cat}/K_m = 9.3 \times 10^4\,M^{-1}s^{-1}$. Meanwhile, antibody 6G6, raised against the transition state analog **36** catalyzed the same reaction with a $k_{cat} = 81\,min^{-1}$, $K_m = 890\,\mu M$ at pH 8.0, and $k_{cat}/K_m = 4.5 \times 10^4\,M^{-1}s^{-1}$. The transition state analog approach provided good biocatalysts in terms of turnover numbers and enantiomeric discrimination, albeit with varying degrees of product inhibition by phenol **34**. Reactive immunization has generated biocatalysts that are ultimately more proficient because they combine an efficient 'catalytic' mechanism, improve substrate recognition, and do not suffer from product inhibition. In practice, these hydrolytic antibodies generated by reactive immunization have also been applied to the hydrolysis of polyesters.[67,68]

The reactive immunization strategy has also been successfully utilized in the aldol reaction.[69,70] Two highly efficient aldolase antibodies, 38C2 and 33F12, were elicited by hapten **37**, equipped with a moderately reactive β-1,3-diketone functionality. The β-1,3-diketone moiety demonstrated its distinct ability to trap a lysine side chain amine affording an enaminone **39** through Schiff base **38**, which directly participates in the mechanism of the aldol reaction in the active site of the antibody (Scheme 19a). The two antibodies, 38C2 and 33F12, obtained by reactive immunization performed extraordi-

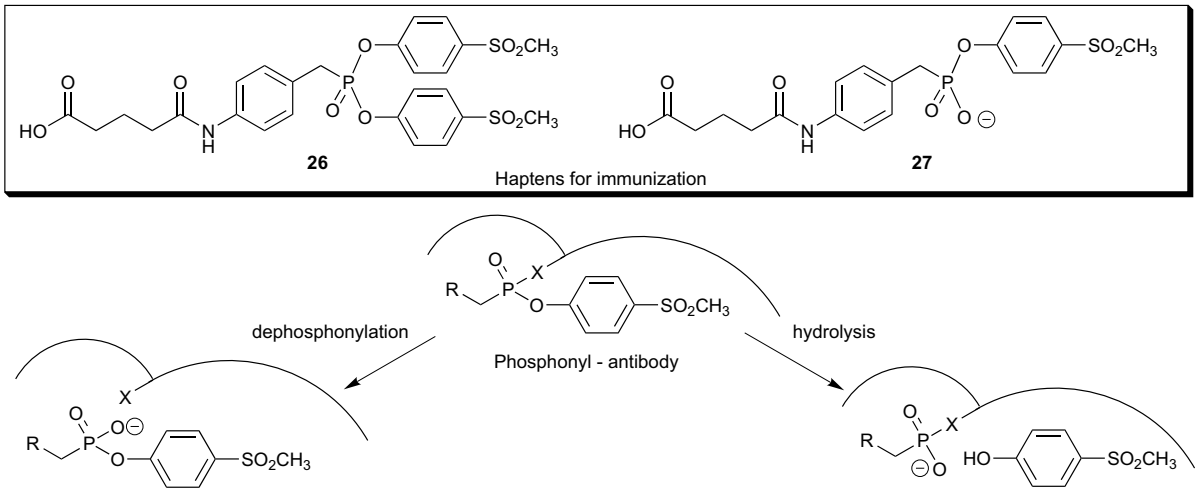


**Scheme 16.** Haptens and chemical opportunities that can take place in the antigen combining site when the antibody reacts with the phosphonate diester. X = a nucleophile in the antibody.

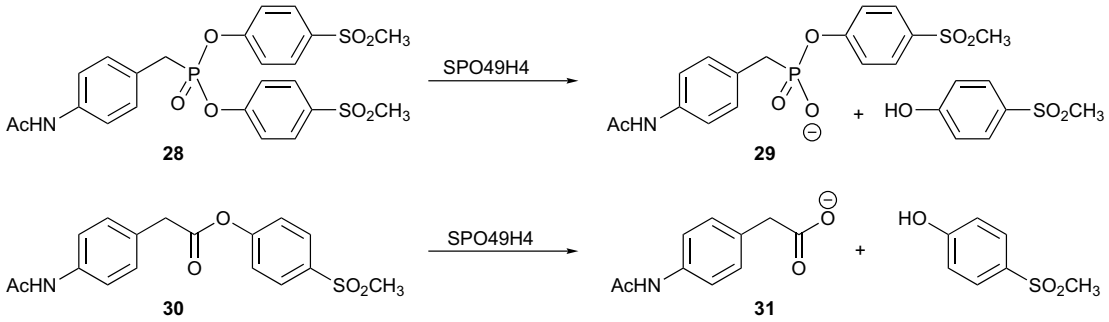


**Scheme 17.** Reactions catalyzed by catalytic Ab SPO49H4.

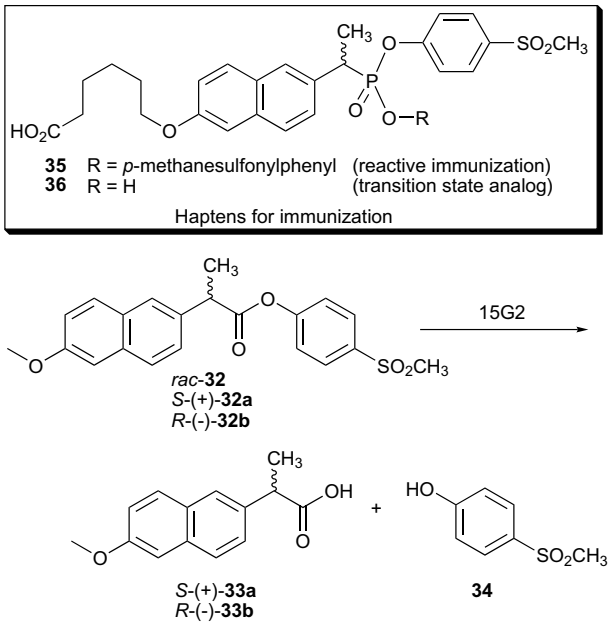


**Scheme 18.** Kinetic resolution by catalytic antibodies, and phosphonate diester **35** and monoester **36** as haptens.

nary catalysis of the aldol reaction between acetone and the aldehyde **40**, with catalytic proficiency, $(k_{cat}/K_m)/k_{uncat}$ of nearing $10^9$ (Scheme 19b). The X-ray structure of 33F12 revealed that the catalytic mechanisms of this antibody is significantly dependent on $Lys^{H93}$, which initiates catalysis by forming a stable covalent conjugated enamine with the ketone substrate that becomes the aldol donor. These two aldolases are shown to be extremely robust and have participated in major steps of the total synthesis of epothilones A–F.[71,72]

In the search for improved aldolase antibodies, Zong et al. employed reactive immunization in combination with transition state theory.[73] On the basis of hapten **37**, a hybrid, hapten **42**, was designed, recruiting not only a sulfone functionality to establish the tetrahedral motif that present in the transition state, but also a β-diketone for trapping a lysine side chain at the active site (Scheme 20).[73] Two aldolase antibodies, 93F3 and 84G3, were isolated. In the aldol reaction of **45** with 3-pentanone, antibody 93F3 provided *syn*-aldol **46** with 90% *de* and 99% *ee*, while antibody 38C2, elicited to hapten **37** afforded only 62% *de* and 59% *ee*. When using these aldolase antibodies for the kinetic resolution of (±)-**47**, antibodies 93F3 and 84G3 showed a $10^3$-fold

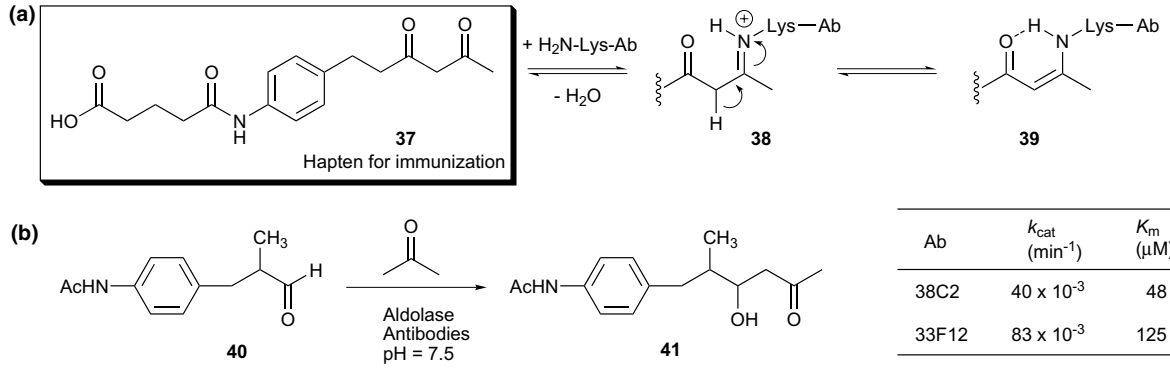


| Ab | $k_{cat}$ ($min^{-1}$) | $K_m$ (μM) |
|---|---|---|
| 38C2 | 40 x $10^{-3}$ | 48 |
| 33F12 | 83 x $10^{-3}$ | 125 |

**Scheme 19.** (a) General mechanism for trapping LysH93 in a catalytic antibody, (b) Aldol reaction catalyzed by mAb38C2 and 33F12.

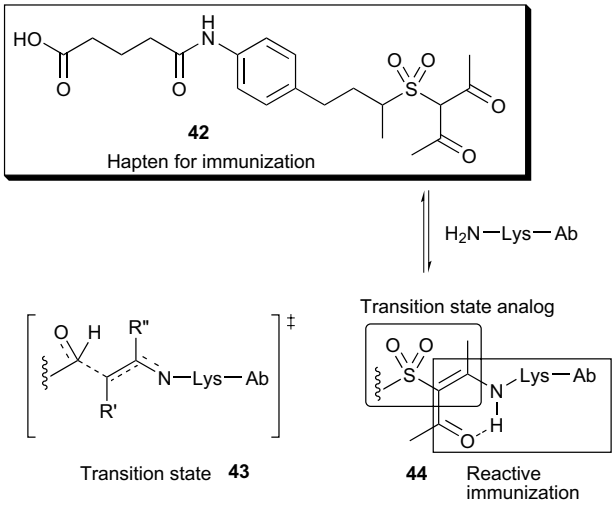


**Scheme 20.** Design of the hybrid hapten **42** from the presumed transition state.

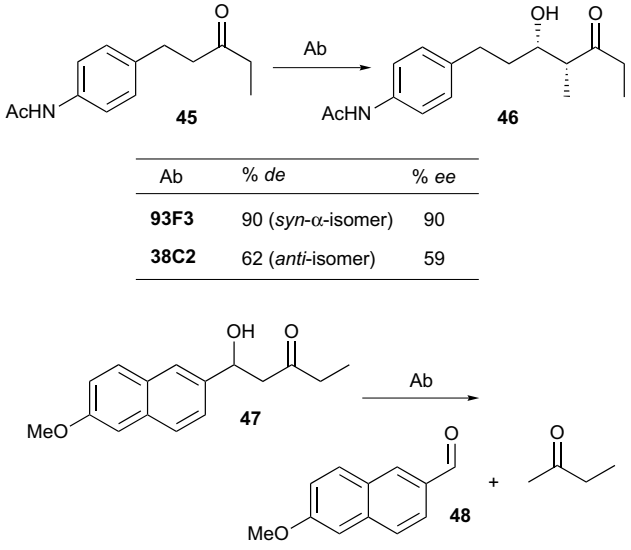


| Ab | % *de* | % *ee* |
|---|---|---|
| **93F3** | 90 (*syn*-α-isomer) | 90 |
| **38C2** | 62 (*anti*-isomer) | 59 |

| Ab | $k_{cat}$ [$min^{-1}$] | $K_m$ [μM] | $k_{cat}/k_{uncat}$ | $(k_{cat}/K_m)/k_{uncat}$ [$M^{-1}$] |
|---|---|---|---|---|
| **93F3** | 43.3 | 6.5 | 4.9 x $10^7$ | 7.4 x $10^{12}$ |
| **84G3** | 46.8 | 10.3 | 5.4 x $10^7$ | 5.0 x $10^{12}$ |
| **38C2** | 0.05 | 29.5 | 5.8 x $10^4$ | 2.0 x $10^9$ |

**Scheme 21.** Comparison between 93F3, 84G3, and 38C2 for aldol and retro-aldol reactions.

increase in proficiency over the antibody 38C2 (Scheme 21).

Taking advantage of insights gained by existing aldolases 38C2 and 33F12, obtained by reactive immunization, a V gene shuffling strategy was established by Tanaka et al. for the reconstruction of aldolase antibodies with improved substrate specificity and turnover.[74] The crystal structure of antibody 33F12 revealed that sequences of the LysH93, HCDR3, and LCDR3 are critical with respect to the mechanism of catalysis, as well as the hydrophobic nature of the combining sites. These sequences were therefore retained when constructing an antibody heavy chain variable domain library using human bone marrow cDNA. The phage displayed libraries were screened against 1, 3-diketone **51**-, and **37**-BSA in order to select antibodies that would tolerate substrates **49** and **50** (Scheme 22). The phage-selected clones were further screened by ELISA to identify soluble Fab capable of binding both **37** and **51**. The last stage of selection, which utilized fluorogenic substrates **52**–**54** (Scheme 23), identified antibody Fab 28. Though the catalytic mechanism of parental antibodies appeared to be conserved in Fab 28-catalyzed reactions, the $K_{cat}$ values of this antibody were superior relative to those of the parental antibodies for the same substrates, approximately 3–10-fold higher.

Mechanism-based inhibitors covalently react with the active site in target proteins and inhibit their activities, they therefore provide a wealth of information to guide the design of immunogens for immunization.[75–77] For example, penam sulfones have been shown to be potent mechanism-based inhibitors of β-lactamase by forming an acyl-enzyme intermediate, which inspired the design of the sulfone hapten **55** targeting the hydrolysis of the lactam functionality built in the substrate **56**.[78] Immunoconjugate **55**-KLH immunized, and a scFv library was constructed using the spleen cells of immunized mice. Screening of the library afforded two scFv antibodies, FT6 and FT12; these antibodies catalyzed hydrolysis of **56** with rate accelerations ($k_{cat}/k_{uncat}$) of 5200 and 320, respectively (Scheme 24).

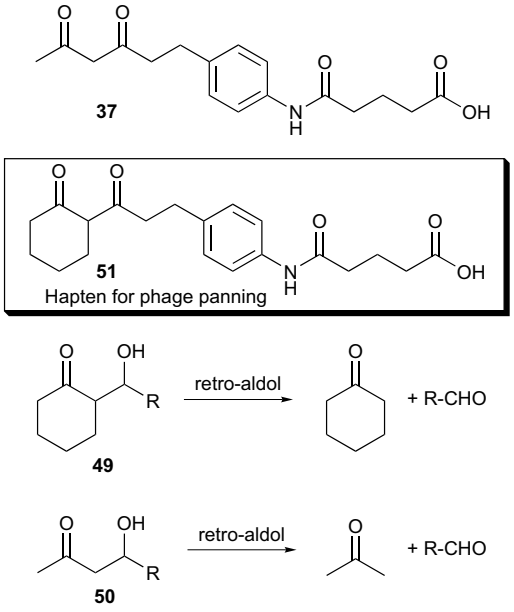


**Scheme 22.** Retro-aldol reactions; the new hapten **51** and original hapten **37**.

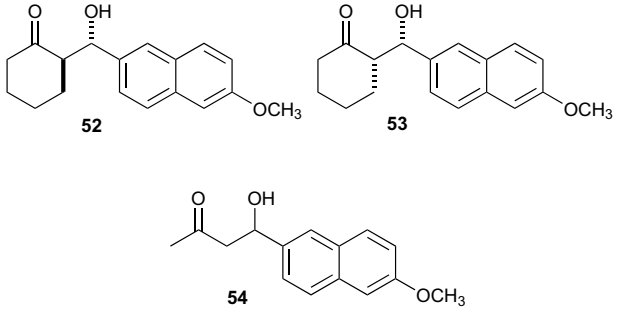


**Scheme 23.** Substrates for a retro-aldol reaction catalyzed by Fab 28.

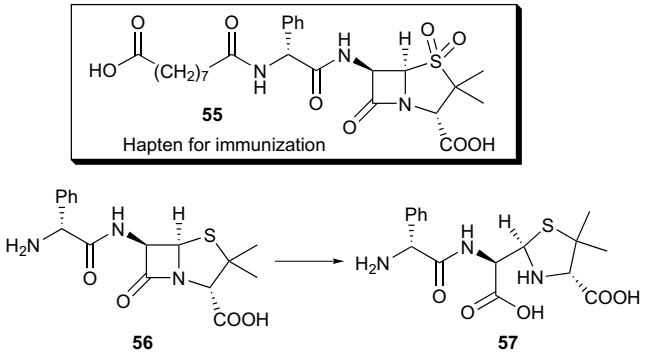


**Scheme 24.** Reactive hapten **55** and reaction catalyzed by catalytic antibody.

## 2.4. Cofactor approaches

Metal-coordinated enzymes are ubiquitous in nature. A metallic species at the active site of an enzyme often plays a critical role in the reaction pathway by enhancing substrate selectivity and accelerating reaction rates. In the field of catalytic antibodies, substantial effort has been directed toward the development of improved antibody catalysts that recruit metals at the active site.

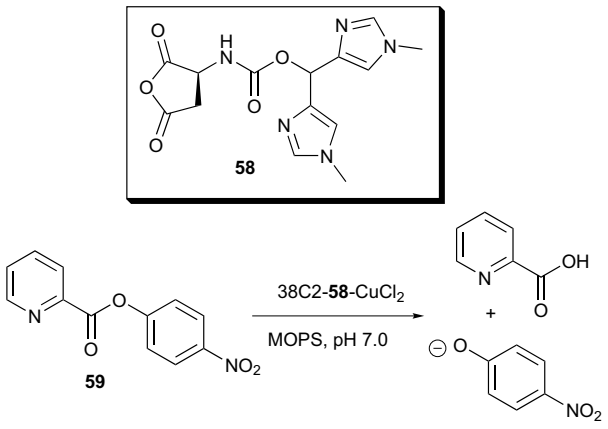


**Scheme 25.** Cofactor **58** and hydrolysis of **59** by 38C2-**58**-$CuCl_2$.

Antibody aldolase 38C2 was chosen as the parent antibody by several groups for the development of novel catalytic antibodies by the recruitment of cofactors. Nicholas et al. have employed bis-imidazolyl ligand coordinated copper complexes a cofactor, taking advantage of the high copper binding affinity ($K_d \sim 10^{-12}$) of the ligand (Scheme 25).[79,80] Insertion of this cofactor was achieved by the coordination of residue $Lys^{H93}$ with **58**, which was equipped with a reactive succinic anhydride moiety and $CuCl_2$. This semisynthetic metalloantibody, 38C2-**58**-$CuCl_2$, catalyzed the hydrolysis of picolic acid ester **59** in aqueous buffer under physiological conditions. This study exemplified that modification of the active site by a metal-coordinated ligand could alter the catalytic nature of the parent antibody, affording a catalyst with very different catalytic activity.

Incorporation of metallic cofactors demonstrated the potential to change not only the function of catalytic antibodies, but also to improve the parent antibody regarding substrate selectivity, turnover, and efficiency, while retaining the same catalytic mechanism. For example, when palladium(II), Pd(en)$Cl_2$ or $Na_2PdCl_2$ was added to aldolase antibodies 38C2 and 33F2, their reaction rates were accelerated.[81] Notably, Pd(en)$Cl_2$-antibody binding is reversible, and enantioselectivity was improved in the case of 38C2 by addition of Pd(II) (Scheme 26). Other than metallic cofactors, external nucleophilic cofactors could also be employed to improve the catalytic activity of the catalytic antibodies. Using excess phenol as the cofactor, the three antibodies, elicited to homologous and heterologous immunization with haptens **60** and **61**, accelerated the cleavage of propionyl *p*-nitroanilide (Scheme 27).[82,83]

Pyridoxal 5′-phosphate (PLP, **62**) has been shown to be an effective cofactor for antibody-catalyzed aldol and retro-aldol reactions.[84] Aldolase antibody 10H2, elicited to hapten **63**, catalyzed the aldol reaction between glycine and aldehyde **64**, when combined with cofactor

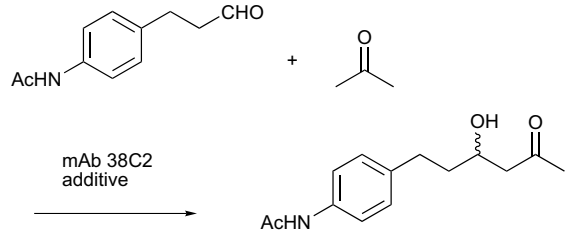


| additive | conc. (μM) | $k_{cat}$ ($min^{-1}$) | $K_m$ (μM) |
|---|---|---|---|
| none | | $4.3 \times 10^{-3}$ | 18.0 |
| $VOSO_4$ | 100 | $3.1 \times 10^{-3}$ | 11.6 |
| $Na_2PdCl_4$ | 15 | $6.1 \times 10^{-3}$ | 27.7 |
| $Pd(en)Cl_2$ | 15 | $6.6 \times 10^{-3}$ | 28.4 |

**Scheme 26.** Effect on retro-aldol reaction by 38C2 with additives.

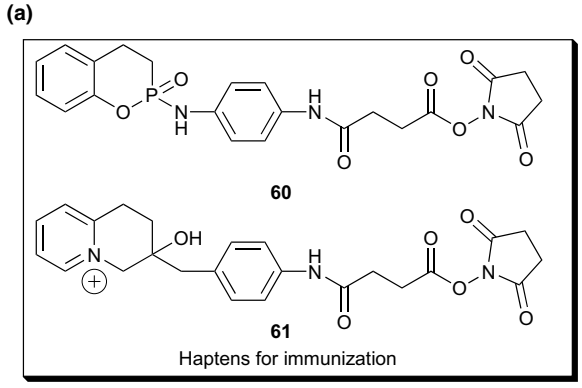


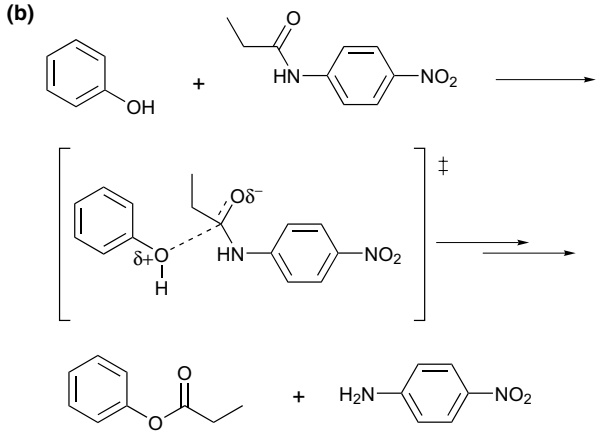


(c)

| catalytic antibody | haptens | immuniza-tion | app $k_{cat}$[a] ($10^{-5}/min^{-1}$) | $K_m^{phenol}$ (μM) | $K_m^{substrate}$ (μM) |
|---|---|---|---|---|---|
| 6-17 | 60/60/60 | homologous | 2.1 | 78 | 310 |
| 3-49 | 61/61/61 | homologous | 1.3 | 14 | 77 |
| 14-10 | 60/60/61 | heterologous | 13.3 | 136 | 370 |

[a] The $K_{cat}$ value were measured by holding the phenol concentration in excess (pseudo-first-order rate constants)

**Scheme 27.** (a) Haptens **60** and **61**, (b) proposed catalytic mechanism and (c) effect of homologous and heterologous immunization.

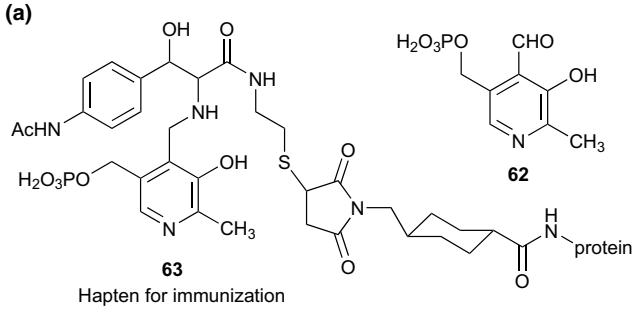


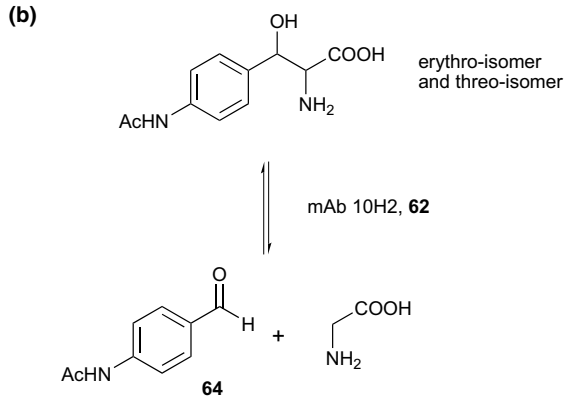


**Scheme 28.** (a) Structure of PLP **62** and hapten **63** conjugated to carrier protein, (b) aldol and retro-aldol reactions catalyzed by mAb 10H2 with PLP **62**.

PLP **62**, with a rate acceleration of double the background reaction where no PLP was applied. (Scheme 28a).[85] This incorporation of PLP also improved the rates of the retro-aldol reactions of the *threo*- and *erythro*- isomers with rate enhancements of 4-fold and 2.5-fold, respectively (Scheme 28b).

Metalloporphyrins have attracted great interest in the research field of biological oxidation processes; its application as a cofactor for a catalytic antibody was recently investigated.[86–88] Antibody SN37.4, elicited against a water soluble tin(IV) porphyrin **65** exhibited desired oxidative activity upon assembly with a ruthenium(II) cofactor **66**, transferring oxygen to substrate **67** (Scheme 29).[89] This antibody-metalloporphyrin assembly featured typical enzyme characteristics regarding substrate selectivity, enantioselective oxygen delivery, and saturation kinetics.

## 2.5. Other approaches

To improve the substrate specificity of catalytic antibodies, a new modular assembly strategy has been developed, which relies on the assembly of a small peptide with enzyme-like qualities by combining a known catalytic peptide and fluorescein-binding peptide (Scheme 30).[90] A 24-amino acid residue peptide (FT-YLK3; YKLLKELLAKLKWLLRKLLGPTCL) has been shown to catalyze the retro-aldol reaction, albeit with relatively poor substrate affinity ($K_m = 1.8$ mM).[91] In other work, a small 12-amino acid residue peptide (FluS303; YPNEFDWWDYYY) was identified as a

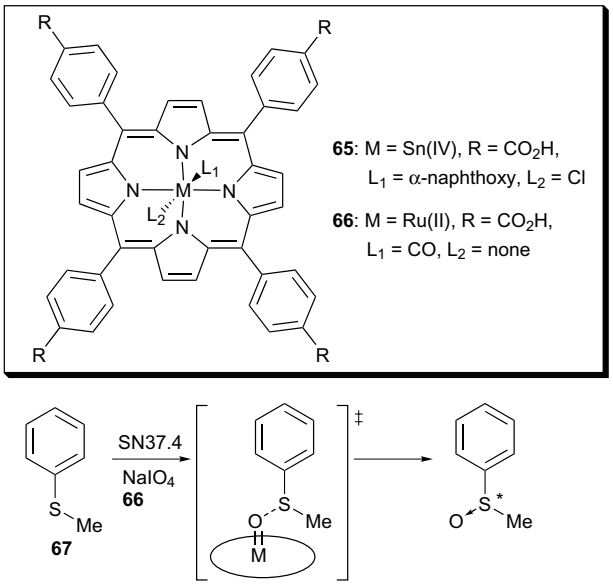


**Scheme 29.** Haptens and proposed oxidation mechanism.

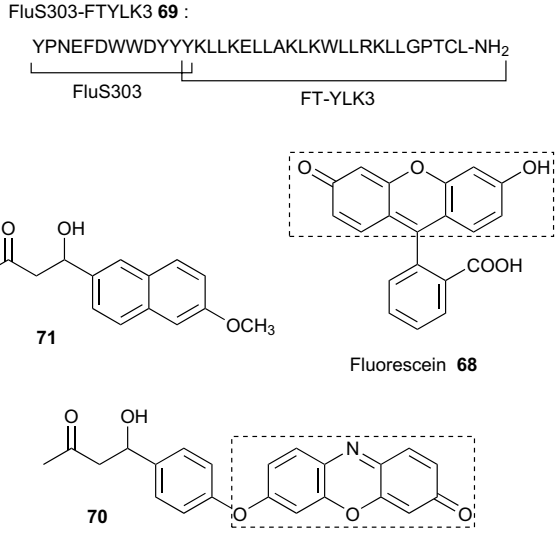


**Scheme 30.** Fused peptide **69**, fluorescein **68**, substrate **70** and **71**.

binder for small molecule fluorophore **68**.[92] These two peptides were covalently linked to afford peptide FluS303-FTYLK3 **69**, which catalyzed the retro-aldol reaction of **70** equipped with a moiety similar to fluorophore **68**, with a $K_m$ of 8 μM and a $k_{cat}$ of $2.3 \times 10^{-4}$ min$^{-1}$. Substrate **71**, a similar hapten without the fluorophore moiety, was also applied in order to examine the substrate recognition of the peptide FTYLK3. The 4-fold higher rate acceleration of peptide-catalyzed retro-aldol reaction of **70** relative to that of **71** indicated improved substrate specificity.

In the process of eliciting antibodies capable of hydrolyzing cocaine, Janda and co-workers underscored the importance of the linker moiety in haptenic structures with regard to immunogenicity.[93] In these studies, immunogen GNP**72** and GNL**73** were carefully evalu-

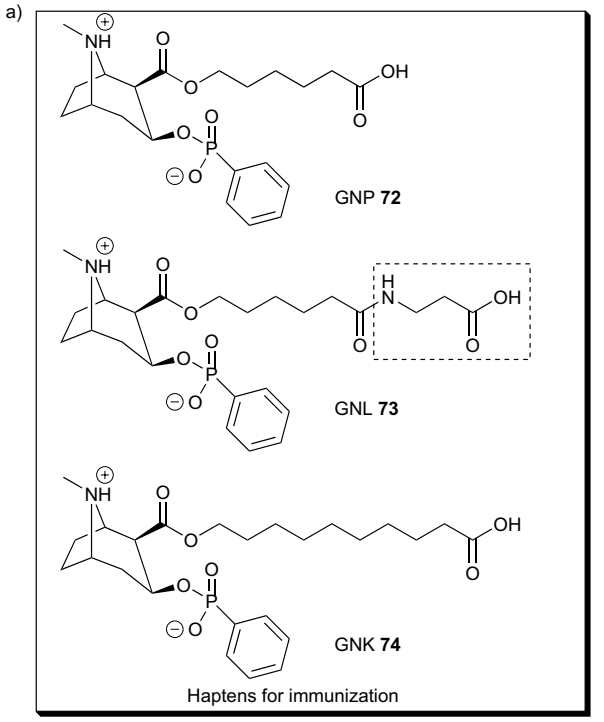


c) Data for some catalytic mAbs that hydrolyze cocaine

| mAb | $k_{cat}$ (min$^{-1}$) | $K_m$ (μM) | $K_{cat}/K_m$ (M$^{-1}$s$^{-1}$) | $K_{cat}/k_{uncat}$ |
|---|---|---|---|---|
| GNL3A6 | 0.030 | 55 | 9.2 | 3705 |
| GNL4D3 | 0.010 | 70 | 2.3 | 1210 |
| GNL23A6 | 0.038 | 830 | 0.77 | 4690 |
| GNK28C9 | 0.0060 | 2080 | 0.050 | 745 |

Determined in 100 mM phospate buffer, pH7.4, 21 °C

**Scheme 31.** (a) Transition-state analog haptens **72**, **73**, and **74**. (b) Reaction and (c) data for some catalytic mAbs that hydrolyze cocaine.

ated (Scheme 31). GNP **72** employed a short linker for conjugation with carrier proteins. In comparison, the linker moiety of GNL **73** is extended by addition of a β-alanine. Surprisingly, this simple change in the linker structure imposed dramatically different immune responses during immunization. Conjugate **72**-KLH afforded no antibodies with desired catalytic activity, while conjugate **73**-KLH successfully elicited several antibody catalysts, such as GNL3A6, GNL4D3, and GNL23A6 (Scheme 31b,c). To fully investigate the importance of linker moiety, Janda et al. designed a third hapten, GNK **74**, which is equipped with a linker of the same length as the one in **73** but without the amide functionality (Scheme 31a). During immunization of **74**-KLH, even though antibodies with catalytic

capacity were obtained, they demonstrated a much lower activity. It was suggested that both the length of the linker and the precise position of the internal amide bond within the linker structure are required for a hapten to adequately trigger the defense mechanism of the adaptive immune system.

## 3. Screening strategies for detection of catalytic antibodies

In order to exploit the full power of the combinatorial system of catalytic antibodies, direct selection strategies for function are needed. One common screening method has been established by Tawfik et al., which is termed catELISA (Scheme 32).[94] Compared to traditional ELISA (enzyme-linked immunosorbent assay), which detects the binding of a substrate, catELISA relies on recognition of the reaction products. Though catELISA has been widely applied in the research of catalytic antibodies, the fact that it requires the use of a product-binding antibody significantly impedes the further generality of this approach.

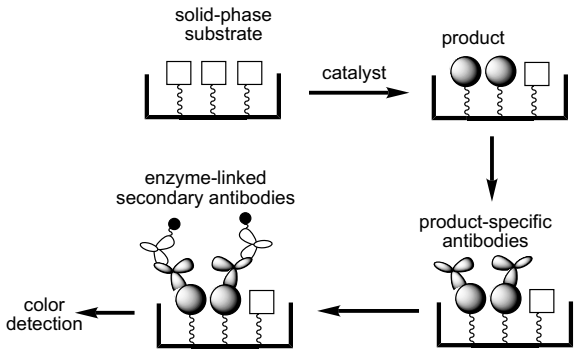


**Scheme 32.** catELISA.

Amongst numerous methods developed to date, efficient utilization of spectroscopic assays is one of the most straightforward methods for the identification and selection of catalytic antibodies. Ellman's reagent (DTNB, 5,5′-dithiobis(2-nitrobenzoic acid) is one of the oldest and most reliable reagents for the detection and quantification of free sulfhydryl content in peptides and proteins. Cashman et al. has reported the application of Ellman's reagent in high-throughput screening of hybridoma cultures obtained from immunization with a transition state analog **75**. This TSA is a non-natural cocaine derivative with the opposite configuration of the benzoyl ester at the C-3 position relative to natural cocaine (Scheme 33a).[95,96] In their studies, thiol liberated upon antibody-catalyzed cleavage of the benzoylthiolester **75** reacted with Ellman's reagent (DTNB) affording spectroscopically detectable TNB (Scheme 33b). This approach is advantageous in that antibody catalysts can be rapidly identified without extraction or derivatization. Notably, the synthesis of cocaine benzoylthiolester **76**, which is equipped with the same stereochemistry as natural cocaine, was recently reported by Janda and co-workers[97] The higher fidelity substrate enabled the determination of cocaine hydrolysis by catalytic antibodies using a spectroscopic assay.

A number of sensor-based assays have also been developed to monitor catalytic reactions using fluorogenic or chromogenic compounds. The application of these compounds provides not only a simple and sensitive assay system but also potential applications in high-throughput screening for the identification of useful biocatalysts.

In 1999, Reymond and co-workers established a high-throughput screening protocol for the discovery of a retro-Diels–Alderase.[98] Substrate **77** incorporated a fluorogenic moiety masked by surrounding structural components. During the course of antibody-catalyzed retro-Diels–Alder reaction, strong blue fluorescence

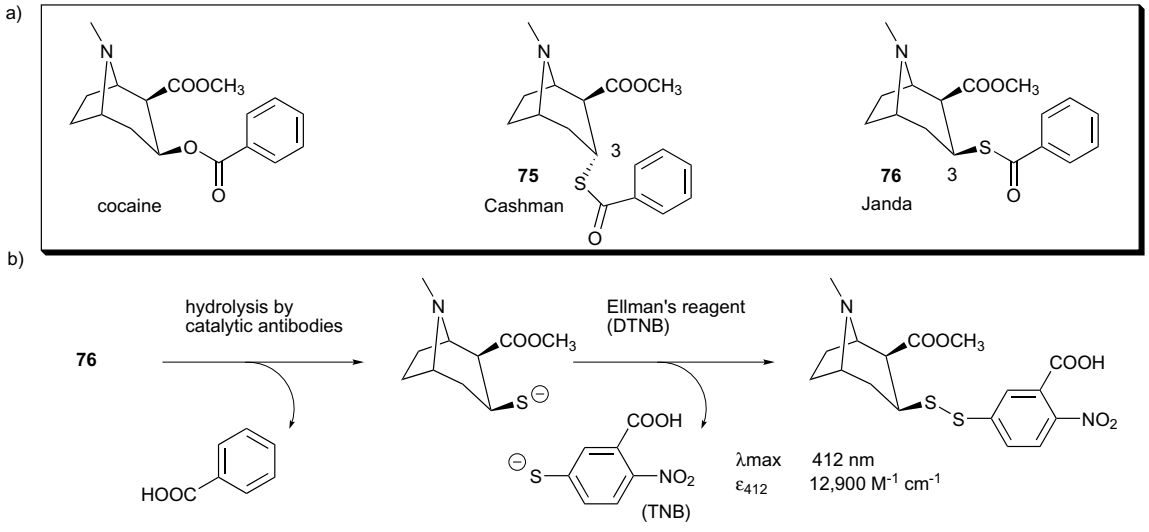


**Scheme 33.** (a) Structures of cocaine and cocaine benzoyl thioesters. (b) Screening of antibody catalyzed hydrolysis by using cocaine benzyl thioester with Ellman's reagent.

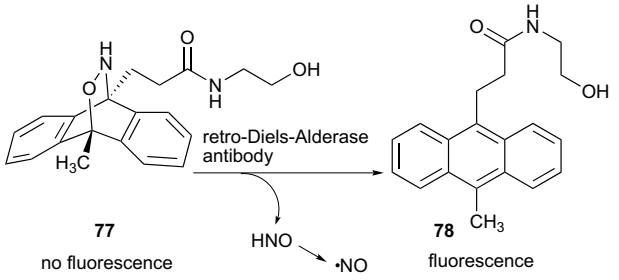


**Scheme 34.** Schematic explanation for the screening of retro-Diels–Alderase antibodies.

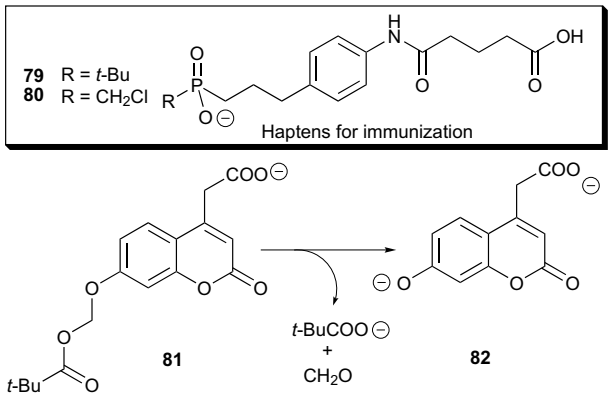


**Scheme 35.** Haptens **79**, **80** and screening method for pivalase antibodies.

was emitted by the product **78** (Scheme 34). This method is independent of pH (between the range of 4 to 8), as well as most buffers or co-solvents. According to the report, more than 14,000 hybridoma cell cultures could be screened using this protocol.

Pivalase catalytic antibodies showed great potential in pro-drug activation (Scheme 35);[99,100] to generate these antibodies Reymond and co-workers employed haptens **79** and **80** for immunization. In the screening stage, a practical method for detection of the antibody catalysts was developed using substrate **81**, a hindered and less reactive ester, which was considered valuable to mitigate background hydrolysis. When the reaction proceeds, **82**-a strongly fluorescent umbelliferone-was liberated, signaling the antibody-catalyzed process. This approach allowed the selection of isolation eleven pivalase antibodies with rate accelerations ($k_{cat}/k_{uncat}$) of ca.$10^3$.

Screening assays for aldolase or retro-aldolase antibodies have been developed taking advantage of a known aldolase antibody 38C2. One of these methodologies requires the employment of umbelliferone **85** in the substrate structure (Scheme 36a).[101,102] When 38C2 was applied to initiate the reaction, masked substrate **83** released the unstable aldehyde **84**, which rapidly rearranged to **85**, emitting strong blue fluorescence, via a β-elimination. A similar substrate **86** containing a masked resorufin was also applied. Upon antibody-

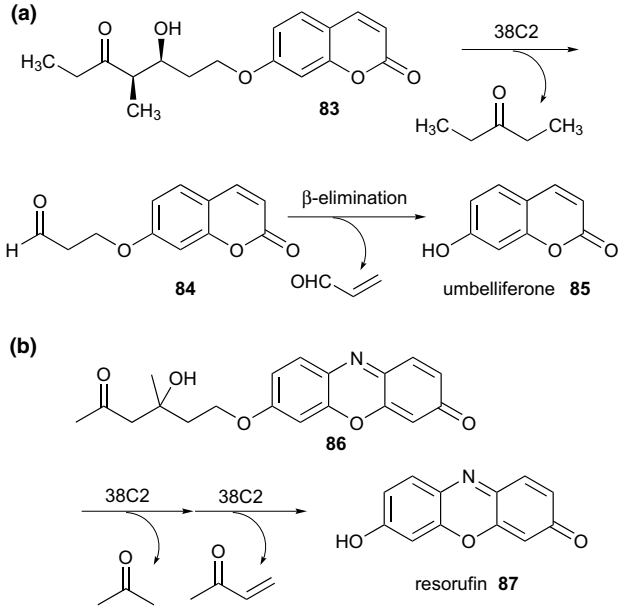


**Scheme 36.** Detection of catalysts for retro aldol-retro-Michael reactions.

catalyzed retro-aldol-retro-Michael reaction, this substrate released **87**, emitting a strong red fluorescent (Scheme 36 b).[103]

As an alternate approach, a detection system has been developed using substrate **88**, which does not contain a masked fluorogenic moiety.[104] When treated with antibody aldolase 38C2, compound **89** was generated, which readily reacts with commercially available diazonium salts in PBS buffer (pH 7.4) affording a color change (Scheme 37). Among the five diazonium salts tested in this study, Fast Red TR salt, **90**, was found to be the

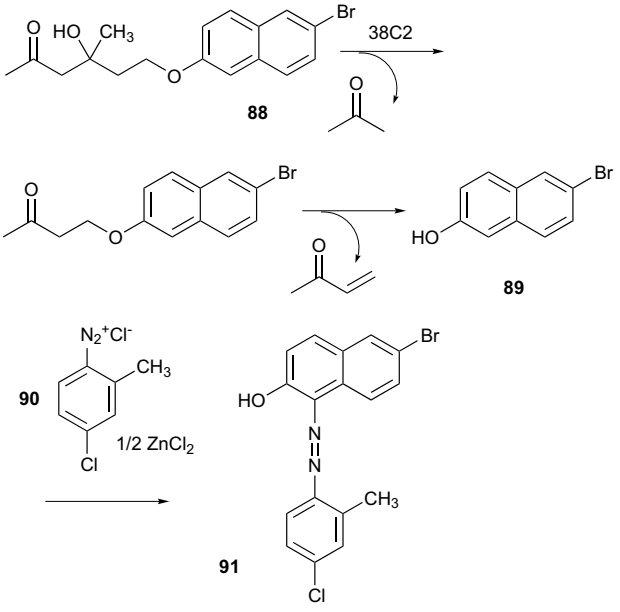


**Scheme 37.** Screening of aldolase antibodies using diazonium salt **90**.

most effective, giving a bright red color when reacted with **89**. As a different approach to test this screening system, substrate **88** was mixed with 38C2 hybridoma cell culture; after incubation at 37 °C for 17 h, this media turned red compared to the negative control using hybridoma cells of noncatalytic antibodies.

Recently, a novel assay that detects C–C bond formation directly was reported, which does not require the use of masked fluorogenic or chromogenic substrates. Substrate **92**, which is known for its application in the analysis of C–S bond formation,[105–107] was used in this assay system to detect C–C bond formation (Scheme 38).[108,109] When the target Michael addition takes place, product **93** (1 μM) demonstrated approximately 100-fold higher fluorescence intensity than that of **92** (1 μM) at $\lambda_{em} = 365$ nm in pH 7 buffer under $\lambda_{ex} = 315$ nm. This assay tolerates a broad pH range and many organic solvents, and is therefore a valuable method for the identification and evolution of new biocatalysts for both the Michael addition and Diels–Alder reaction.

In the last decade, the use of combinatorial libraries displayed on phage has emerged as a powerful tool for the screening of catalytic antibodies. Despite the advantages of this approach, including the absence of animal requirements and vastly reduced timeframe, it remains a challenging task to isolate antibodies from these highly diverse libraries. To address this problem, Janda et al. established a direct phage screening system in the search for the galactopyranosidase antibodies.[110] Following the glucosyl bond cleavage of **94**, a fluoride elimination spontaneously took place to yield quinone methide **97**, which, upon encountering reactive antibodies displayed on phage, would trap these antibody in a covalent fashion (Scheme 39a).[111] Nonbinders were simply removed by washing with buffer and acid, while the trapped antibody Fabs were eluted with DTT and amplified through infection with *E. coli*. After repeating this cycle several times, galactopyranosidase antibody Fab 1B was uncovered from a large library of Fab antibodies. Fab 1B catalyzed the hydrolysis of *p*-nitrophenyl β-galactopyranoside with $k_{cat} = 0.007\,min^{-1}$ and $K_m = 530\,\mu M$ corresponding to a rate enhancement ($k_{cat}/k_{uncat}$) of $7 \times 10^4$. In comparison, the best catalytic antibody 1F4 elicited to hapten **99** using classic hybridoma screening showed $k_{cat} = 10^{-5}\,min^{-1}$ and $K_m = 330\,\mu M$ and a rate enhancement of only 100-fold.

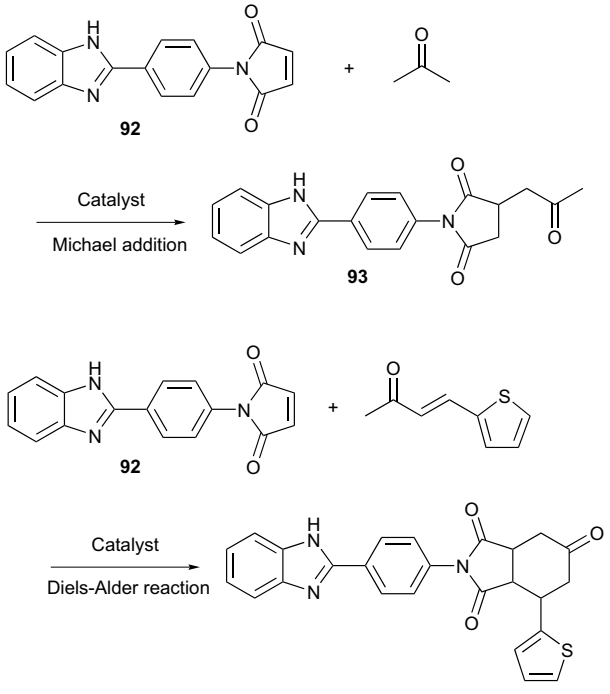


**Scheme 38.** Direct detection of catalysts for Michael addition and Diels–Alder reaction.

This direct screening method is applicable to identify not only galactopyranosidase antibodies but also other protein catalysts. Using a similar protocol, in which ligand **100** was employed as the suicide reagent, Blackburn and co-workers obtained phosphatase antibodies from a highly diverse scFv library.[112,113] scFv TT1 was isolated as a phosphatase-like catalytic antibody after two cycles of panning (Scheme 39b). The catalytic activity of scFv TT1 is two orders of magnitude superior to the best phosphatase antibody, Fab 38E1, reported so far.[114]

A novel trigonal boronic acid hapten **101** has been designed as a transition state analog to elicit antibody catalysts for primary amide bond hydrolysis (Scheme 40).[115] Although no amidase antibody was isolated using hybridoma methodology, Fab-BL25 was uncovered through panning of a combinatorial antibody library displayed on phage. Fab-BL25 performed highly efficient hydrolysis of the terminal primary amide bond in a tripeptide, incorporating regio- and stereoselectivities.

An unavoidable problem inherent in the use of TSAs as haptens is that antibodies are often found to recognize not only the transition state structure, but also other part(s) of the hapten. To minimize the possibility of generating antibodies with undesired specificity, 'short-TSAs', which bear a high degree of structural similarity with the transition state, have been employed in the ELISA screening assay. Using these knowledge, a three-step screening methodology was developed by Nishi and co-workers.[116] In these studies, three transition state analogs were prepared in the search for esterase antibodies, where compound **102** was designed initially for immunization. Structural modifications with regard to the length of the linker moiety as well as the size of the leaving group yielded short-TSAs **103** and **104**, which were used in the later stages of the screening process. As the first step of the screening, antibodies that bind to the full-length TSA **102**-BSA were selected, which was then followed by an ELISA assay for selection of binders to the short TSA **104**-BSA. Lastly, competitive ELISA was performed for the isolation of antibodies that recognize the short TSA **103** (Scheme 41a). The probability of positive hits in each enrichment step was calculated as 22.8%, 45.7%, and 83.3%, respectively. This three-step selection methodology allowed the isolation of 10 monoclonal antibodies that catalyzed the hydrolysis of target ester **105** (Scheme 41b).

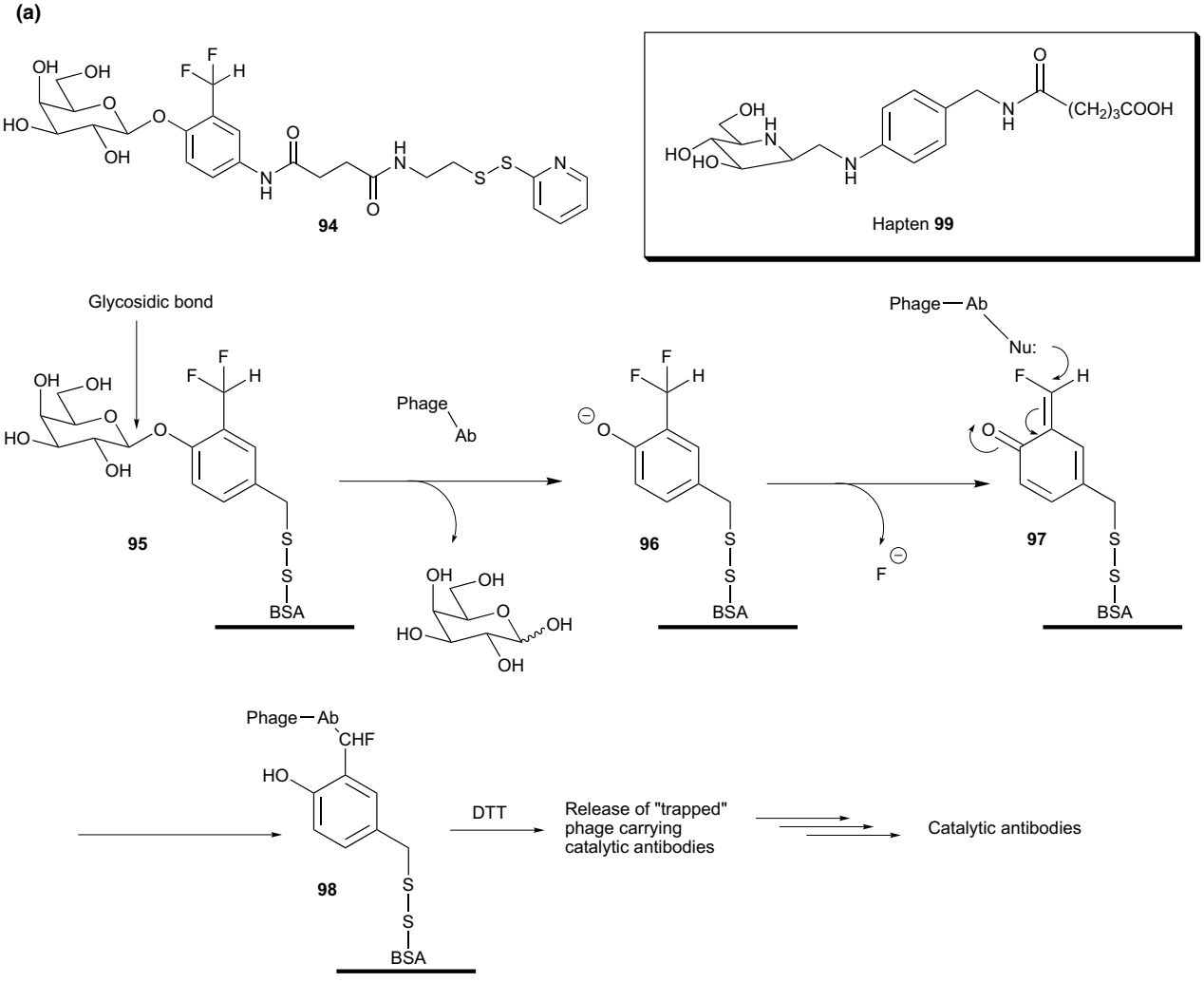


| | $k_{cat}$ ($s^{-1}$) | $k_{cat}/k_{uncat}$ | $K_m$ (μM) | $k_{cat}/K_m$ ($s^{-1}$ $M^{-1}$) | $(k_{cat}/K_m)/k_{uncat}$ ($M^{-1}$) |
|---|---|---|---|---|---|
| scFv TT1 | $5.0 \times 10^{-4}$ | $2.3 \times 10^{5}$ | 46 | 10.9 | $4.9 \times 10^{9}$ |
| IgG or Fab 38E1 | $2.0 \times 10^{-5}$ | $9.0 \times 10^{3}$ | 155 | 0.13 | $5.9 \times 10^{7}$ |

**Scheme 39.** (a) Schematic representation of the screening of catalytic antibodies by direct chemical selection using hapten **99**. (b) Ligand **100** for the screening of phosphatase Abs and comparison between previously reported IgG or Fab 38E1 and scFv TT1 chosen by direct chemical selection.

## 4. Conclusion

Since the first successful examples of tailored antibodies that catalyze chemical transformations, great attention has been drawn to this field of research. In the last two decades, a large number of antibodies that are able to catalyze a variety of chemical processes have been investigated. Based on the concept of catalytic antibodies as first described by Jencks, the use of a transition state analog of the target reaction to elicit antibodies during an immune response has been developed and identified as a classic strategy in the search for catalytic antibodies. The newer established hapten strategies-'bait-and-switch' catalysis and reactive immunization-allow for the recruitment of the desired amino acid functionalities in the catalytic machinery of the antibodies

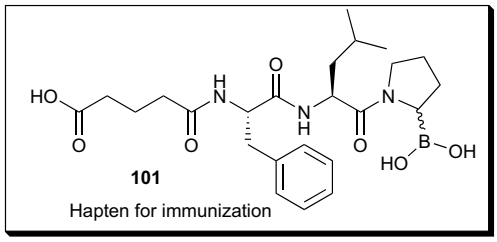


**Scheme 40.** Hapten **101** used for phage display panning toward antibody catalyzed amide bond hydrolysis.

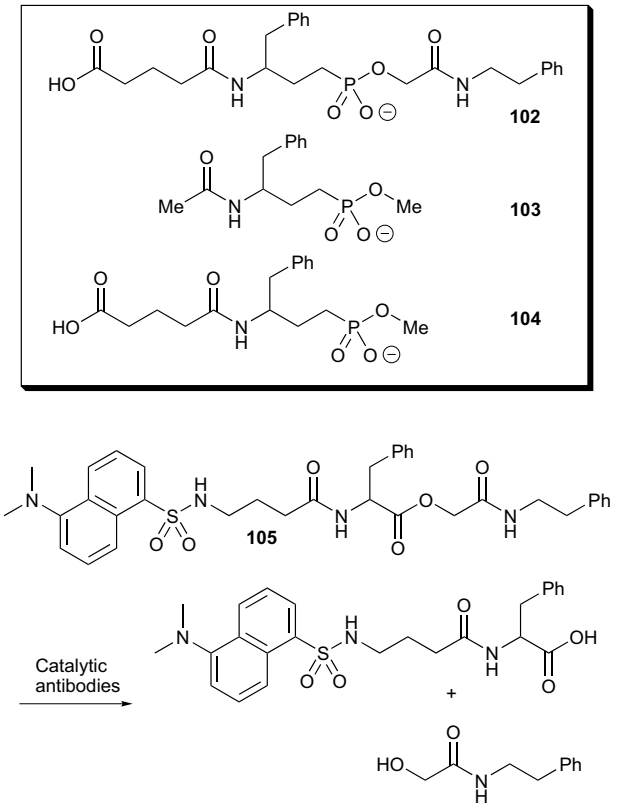


**Scheme 41.** (a) Structure of transition state analogs **102**, **103**, and **104**. (b) Hydrolysis of substrate **105** used for detecting catalysis.

during immunization. Moreover, improved hapten-carrier linkages have been developed that can greatly enhance the immune response to otherwise poorly immunogenic haptens. The application of cofactors has also been shown to be a valuable strategy to yield antibodies with desired catalytic capabilities. Finally, the employments of chemosensor and phage display systems have greatly advanced the efficiency of the screening process for detection of antibody catalysts.

We hope that these advancements, as well as future breakthroughs in this field of research will facilitate the discovery of catalytic antibodies that demonstrate catalytic efficiencies comparable with natural enzymes. Furthermore, we anticipate the generation of more robust antibody catalysts that could provide synthetic chemists with novel tools to target challenging problems.

## Acknowledgements

We thank Jason Moss, Dr. Masayuki Matshushita, Dr. Michael Meijler, and Reshma Jagasia for constructive suggestions and helpful discussions. We are grateful to the National Institutes of Health, the National Institute of Drug Abuse and the Skaggs Institute for Chemical Biology for support of our work in this area.

## References and notes

1. Jencks, W. P. *Catalysis in Chemistry and Enzymology*; McGraw-Hill: New York, 1967.
2. Pollack, S. J.; Jacobs, J. W.; Schultz, P. G. *Science* **1986**, *234*, 1570.
3. Tramontano, A.; Janda, K. D.; Lerner, R. A. *Science* **1986**, *234*, 1566.
4. Eyring, H. *J. Chem. Phys.* **1935**, *3*, 107.
5. Eyring, H. *Chem. Rev.* **1935**, *17*, 65.
6. Tanaka, F. *Chem. Rev.* **2002**, *102*, 4885.
7. Stewart, J. D.; Benkovic, S. J. *Nature* **1995**, *375*, 388.
8. Mader, M. M.; Bartlett, P. A. *Chem. Rev.* **1997**, *97*, 1281.
9. Gao, C. S.; Lavey, B. J.; Lo, C.-H. L.; Datta, A.; Wentworth, P., Jr; Janda, K. D. *J. Am. Chem. Soc.* **1998**, *120*, 2211.
10. Janda, K. D.; Schloeder, D.; Benkovic, S. J.; Lerner, R. A. *Science* **1988**, *241*, 1188.
11. Stewart, J. D.; Krebs, J. F.; Siuzdak, G.; Berdis, A. J.; Smithrud, D. B.; Benkovic, S. J. *Proc. Natl. Acad. Sci. U.S.A.* **1994**, *91*, 7404.
12. Roberts, V. A.; Stewart, J.; Benkovic, S. J.; Getzoff, E. D. *Protein Eng.* **1993**, *6*, 85.
13. Roberts, V. A.; Stewart, J.; Benkovic, S. J.; Getzoff, E. D. *J. Mol. Biol.* **1994**, *235*, 1098.
14. Thayer, M. M.; Olender, E. H.; Arvai, A. S.; Koike, C. K.; Canestrelli, I. L.; Stewart, J. D.; Benkovic, S. J.; Getzoff, E. D.; Roberts, V. A. *J. Mol. Biol.* **1999**, *291*, 329.
15. Chong, L. T.; Bandyopadhyay, P.; Scanlan, T. S.; Kuntz, I. D.; Kollman, P. A. *J. Comput. Chem.* **2003**, *24*, 1371.
16. Aggarwal, R.; Benedetti, F.; Berti, F.; Buchini, S.; Colombatti, A.; Dinon, F.; Galasso, V.; Norbedo, S. *Chem. Eur. J.* **2003**, *9*, 3132.
17. Hasserodt, J.; Janda, K. D.; Lerner, R. A. *J. Am. Chem. Soc.* **1997**, *119*, 5993.
18. Paschall, C. M.; Hasserodt, J.; Jones, T.; Lerner, R. A.; Janda, K. D.; Christianson, D. W. *Angew. Chem., Int. Ed.* **1999**, *38*, 1743.
19. Li, T. Y.; Janda, K. D.; Ashley, J. A.; Lerner, R. A. *Science* **1994**, *264*, 1289.
20. Zhu, X. Y.; Heine, A.; Monnat, F.; Houk, K. N.; Janda, K. D.; Wilson, I. A. *J. Mol. Biol.* **2003**, *329*, 69.
21. Baldwin, J. E. *J. Chem. Soc., Chem. Commun.* **1976**, 734.
22. Baldwin, J. E. *J. Chem. Soc., Chem. Commun.* **1976**, 738.
23. Janda, K. D.; Shevlin, C. G.; Lerner, R. A. *Science* **1993**, *259*, 490.
24. Gruber, K.; Zhou, B.; Houk, K. N.; Lerner, R. A.; Shevlin, C. G.; Wilson, I. A. *Biochemistry* **1999**, *38*, 7062.
25. Sauer, J. *Angew. Chem., Int. Ed. Engl.* **1966**, *5*, 211.
26. Hilvert, D.; Hill, K. W.; Nared, K. D.; Auditor, M. T. M. *J. Am. Chem. Soc.* **1989**, *111*, 9261.
27. Chen, J. G.; Deng, Q. L.; Wang, R. X.; Houk, K. N.; Hilvert, D. *Chembiochem* **2000**, *1*, 255.
28. Kim, S. P.; Leach, A. G.; Houk, K. N. *J. Org. Chem.* **2002**, *67*, 4250.
29. Braisted, A. C.; Schultz, P. G. *J. Am. Chem. Soc.* **1990**, *112*.

30. Ulrich, H. D.; Patten, P. A.; Yang, P. L.; Romesberg, F. E.; Schultz, P. G. *Proc. Natl. Acad. Sci. U.S.A.* **1995**, *92*, 11907.
31. Romesberg, F. E.; Spiller, B.; Schultz, P. G.; Stevens, R. C. *Science* **1998**, *279*, 1929.
32. Zhang, X. Y.; Deng, Q. L.; Yoo, S. H.; Houk, K. N. *J. Org. Chem.* **2002**, *67*, 9043.
33. Ylikauhaluoma, J. T.; Ashley, J. A.; Lo, C. H.; Tucker, L.; Wolfe, M. M.; Janda, K. D. *J. Am. Chem. Soc.* **1995**, *117*, 7041.
34. Heine, A.; Stura, E. A.; Yli-Kauhaluoma, J. T.; Gao, C. S.; Deng, Q. L.; Beno, B. R.; Houk, K. N.; Janda, K. D.; Wilson, I. A. *Science* **1998**, *279*, 1934.
35. Cannizzaro, C. E.; Ashley, J. A.; Janda, K. D.; Houk, K. N. *J. Am. Chem. Soc.* **2003**, *125*, 2489.
36. Shi, Z. D.; Yang, B. H.; Wu, Y. L.; Pan, Y. J.; Ji, Y. Y.; Yeh, M. *Bioorg. Med. Chem. Lett.* **2002**, *12*, 2321.
37. Doering, W. V. E.; Roth, W. R. *Tetrahedron* **1962**, *18*, 67.
38. Dewar, M. J. S.; Wade, L. E. *J. Am. Chem. Soc.* **1977**, *99*, 4417.
39. Ulrich, H. D.; Mundroff, E.; Santarsiero, B. D.; Driggers, E. M.; Stevens, R. C.; Schultz, P. G. *Nature* **1997**, *389*, 271.
40. Mundorff, E. C.; Hanson, M. A.; Varvak, A.; Ulrich, H.; Schulz, P. G.; Stevens, R. C. *Biochemistry* **2000**, *39*, 627.
41. Asada, T.; Gouda, H.; Kollman, P. A. *J. Am. Chem. Soc.* **2002**, *124*, 12535.
42. Rossman, M. G.; Liljas, A.; Branden, C.-I.; Banaszak, L. J. Evolutionary and Structural Relationship Among Dehydrogenases In *The Enzymes*; Academic: New York, 1975; Vol. 11.
43. Schroer, J.; Sanner, M.; Reymond, J. L.; Lerner, R. A. *J. Org. Chem.* **1997**, *62*, 3220.
44. MacBeath, G.; Hilvert, D. *Chem. Biol.* **1996**, *3*, 433.
45. Tramontano, A.; Gololobov, G.; Paul, S. Proteolytic Antibodies: Origins, Selection and Induction. In *Catalytic Antibodies*, 2000; Vol. 77, p 1.
46. Stewart, J. D.; Benkovic, S. J. *Chem.. Soc. Rev.* **1993**, *22*, 213.
47. Patten, P. A.; Gray, N. S.; Yang, P. L.; Marks, C. B.; Wedemayer, G. J.; Boniface, J. J.; Stevens, R. C.; Schultz, G. *Science* **1996**, *271*, 1086.
48. Tramontano, A.; Ivanov, B.; Gololobov, G.; Paul, S. *Appl. Biochem. Biotechnol.* **2000**, *83*, 233.
49. Barbany, M.; Gutierrez-de-Teran, H.; Sanz, F.; Villa-Freixa, J.; Warshel, A. *Chembiochem* **2003**, *4*, 277.
50. Hanson, J. E.; Kaplan, A. P.; Bartlett, P. A. *Biochemistry* **1989**, *28*, 6249.
51. Morgan, B. P.; Scholtz, J. M.; Ballinger, M.; Zipkin, I.; Bartlett, P. A. *J. Am. Chem. Soc.* **1991**, *113*, 297.
52. Wiest, O.; Houk, K. N. *J. Org. Chem.* **1994**, *59*, 7582.
53. Tantillo, D. J.; Houk, K. N. *J. Org. Chem.* **1999**, *64*, 3066.
54. Houk, K. N.; Leach, A. G.; Kim, S. P.; Zhang, X. Y. *Angew. Chem., Int. Ed.* **2003**, *42*, 4872.
55. Blackburn, G. M.; Datta, A.; Denham, H.; Wentworth, P. Catalytic antibodies. In *Advances in Physical Organic Chemistry*, 1998; Vol. 31, p 249.
56. Warshel, A. *Acc. Chem. Res.* **1981**, *14*, 284.
57. Yang, G.; Chun, J.; ArakawaUramoto, H.; Wang, X.; Gawinowicz, M. A.; Zhao, K.; Landry, D. W. *J. Am. Chem. Soc.* **1996**, *118*, 5881.
58. Hilvert, D. *Ann. Rev. Biochem.* **2000**, *69*, 751.
59. Janda, K. D.; Weinhouse, M. I.; Schloeder, D. M.; Lerner, R. A.; Benkovic, S. J. *J. Am. Chem. Soc.* **1990**, *112*, 1274.
60. Wentworth, P.; Liu, Y. Q.; Wentworth, A. D.; Fan, P.; Foley, M. J.; Janda, K. D. *Proc. Natl. Acad. Sci. U.S.A.* **1998**, *95*, 5971.
61. Hasserodt, J.; Janda, K. D.; Lerner, R. A. *Bioorg. Med. Chem.* **2000**, *8*, 995.
62. Goncalves, O.; Dintinger, T.; Lebreton, J.; Blanchard, D.; Tellier, C. *Biochem. J.* **2000**, *346*, 691.
63. Tanaka, F.; Barbas, C. F. *J. Immunol. Methods* **2002**, *269*, 67.
64. Wirsching, P.; Ashley, J. A.; Lo, C. H. L.; Janda, K. D.; Lerner, R. A. *Science* **1995**, *270*, 1775.
65. Lo, C. H. L.; Wentworth, P.; Jung, K. W.; Yoon, J.; Ashley, J. A.; Janda, K. D. *J. Am. Chem. Soc.* **1997**, *119*, 10251.
66. Datta, A.; Wentworth, P.; Shaw, J. P.; Simeonov, A.; Janda, K. D. *J. Am. Chem. Soc.* **1999**, *121*, 10461.
67. Chen, D. W.; Kubiak, R. J.; Ashley, J. A.; Janda, K. D. *J. Chem. Soc., Perkin Trans. 1* **2001**, 2796.
68. Lin, C. H.; Hoffman, T. Z.; Xie, Y. L.; Wirsching, P.; Janda, K. D. *Chem. Commun.* **1998**, 1075.
69. Wagner, J.; Lerner, R. A.; Barbas, C. F. *Science* **1995**, *270*, 1797.
70. Barbas, C. F.; Heine, A.; Zhong, G. F.; Hoffmann, T.; Gramatikova, S.; Bjornestedt, R.; List, B.; Anderson, J.; Stura, E. A.; Wilson, I. A.; Lerner, R. A. *Science* **1997**, *278*, 2085.
71. Sinha, S. C.; Sun, J.; Miller, G. P.; Wartmann, M.; Lerner, R. A. *Chem. Eur. J.* **2001**, *7*, 1691.
72. Rader, C.; Turner, J. M.; Heine, A.; Shabat, D.; Sinha, S. C.; Wilson, I. A.; Lerner, R. A.; Barbas, C. F. *J. Mol. Biol.* **2003**, *332*, 889.
73. Zhong, G. F.; Lerner, R. A.; Barbas, C. F. *Angew. Chem., Int. Ed.* **1999**, *38*, 3738.
74. Tanaka, F.; Lerner, R. A.; Barbas, C. F. *J. Am. Chem. Soc.* **2000**, *122*, 4835.
75. Fisher, J.; Charnas, R. L.; Bradley, S. M.; Knowles, J. R. *Biochemistry* **1981**, *20*, 2726.
76. Brenner, D. G.; Knowles, J. R. *Biochemistry* **1981**, *20*, 3680.
77. Silverman, R. B. In *Mechanism-based Enzyme Inactivation: Chemistry and Enzymology*; CRC, 1988; Vol. 1.
78. Tanaka, F.; Almer, H.; Lerner, R. A.; Barbas, C. F. *Tetrahedron Lett.* **1999**, *40*, 8063.
79. Nicholas, K. M.; Wentworth, P.; Harwig, C. W.; Wentworth, A. D.; Shafton, A.; Janda, K. D. *Proc. Natl. Acad. Sci. U.S.A.* **2002**, *99*, 2648.
80. Tanaka, F.; Lerner, R. A.; Barbas, C. F. *Chem. Commun.* **1999**, 1383.
81. Finn, M. G.; Lerner, R. A.; Barbas, C. F. *J. Am. Chem. Soc.* **1998**, *120*, 2963.
82. Ersoy, O.; Fleck, R.; Sinskey, A.; Masamune, S. *J. Am. Chem. Soc.* **1996**, *118*, 13077.
83. Ersoy, O.; Fleck, R.; Sinskey, A.; Masamune, S. *J. Am. Chem. Soc.* **1998**, *120*, 817.
84. Tanaka, F.; Oda, M.; Fujii, I. *Tetrahedron Lett.* **1998**, *39*, 5057.
85. Kimura, T.; Vassilev, V. P.; Shen, G.-J.; Wong, C.-H. *J. Am. Chem. Soc.* **1997**, *119*, 11734.
86. Cochran, A. G.; Schultz, P. G. *Science* **1990**, *249*, 781.
87. Cochran, A. G.; Schultz, P. G. *J. Am. Chem. Soc.* **1990**, *112*, 9414.
88. Harada, A.; Fukushima, H.; Shiotsuki, K.; Yamaguchi, H.; Oka, F.; Kamachi, M. *Inorg. Chem.* **1997**, *36*, 6099.
89. Nimri, S.; Keinan, E. *J. Am. Chem. Soc.* **1999**, *121*, 8978.
90. Tanaka, F.; Barbas, C. F. *J. Am. Chem. Soc.* **2002**, *124*, 3510.
91. Tanaka, F.; Barbas, C. F. *Chem. Commun.* **2001**, *9*, 769.
92. Rozinov, M. N.; Nolan, G. P. *Chem. Biol.* **1998**, *5*, 713.
93. Matsushita, M.; Hoffman, T. Z.; Ashley, J. A.; Zhou, B.; Wirsching, P.; Janda, K. D. *Bioorg. Med. Chem. Lett.* **2001**, *11*, 87.

94. Tawfik, D. S.; Green, B. S.; Chap, R.; Sela, M.; Eshhar, Z. *Proc. Natl. Acad. Sci. U.S.A.* **1993**, *90*, 373.
95. Cashman, J. R.; Berkman, C. E.; Underiner, G. E. *J. Parmacol. Exp. Ther.* **2000**, *293*, 952.
96. Cashman, J. R.; Berkman, C. E.; Underiner, G.; Kolly, C. A.; Hunter, A. D. *Chem. Res. Toxicol.* **1998**, *11*, 895.
97. Isomura, S.; Hoffman, T. Z.; Wirsching, P.; Janda, K. D. *J. Am. Chem. Soc.* **2002**, *124*, 3661.
98. Bensel, N.; Bahr, N.; Raymond, M. T.; Schenkels, C.; Reymond, J. L. *Helv. Chim. Acta* **1999**, *82*, 44.
99. Reymond, J. L. *J. Immunol. Methods* **2002**, *269*, 125.
100. Bensel, N.; Reymond, M. T.; Reymond, J. L. *Chem. Eur. J.* **2001**, *7*, 4604.
101. Jourdain, N.; Carlon, R. P.; Reymond, J. L. *Tetrahedron Lett.* **1998**, *39*, 9415.
102. Wahler, D.; Reymond, J. L. *Canidian. Journal of Chemistry-Revue Canadienne De Chimie* **2002**, *80*, 665.
103. List, B.; Barbas, C. F., III; Lerner, R. A. *Proc. Natl. Acad. Sci. U.S.A.* **1998**, *95*, 15351.
104. Tanaka, F.; Kenwin, L.; Kubitz, D.; Lerner, R. A.; Barbas, C. F., III. *Bioorg. Med. Chem. Lett.* **2001**, *11*, 2983.
105. Sekine, T.; Kanaoka, Y.; Ando, K.; Machida, M. *Anal. Biochem.* **1972**, *48*, 557.
106. Kanaoka, Y.; Machida, M.; Ando, K.; Sekine, T. *Biochim. Biophys. Acta* **1970**, *207*, 269.
107. Kanaoka, Y. *Angew. Chem., Int. Ed. Engl.* **1977**, *16*, 137.
108. Tanaka, F.; Thayumanavan, R.; Barbas, C. F. *J. Am. Chem. Soc.* **2003**, *125*, 8523.
109. Mase, N.; Tanaka, F.; Barbas, C. F. *Org. Lett.* **2003**, *5*, 4369.
110. Janda, K. D.; Lo, L. C.; Lo, C. H. L.; Sim, M. M.; Wang, R.; Wong, C. H.; Lerner, R. A. *Science* **1997**, *275*, 945.
111. Halazy, S.; Berges, V.; Erhard, A.; Danzin, C. *Bioorg. Chem.* **1990**, *18*, 330.
112. Betley, J. R.; Cesaro-Tadic, S.; Mekhalfia, A.; Rickard, J. H.; Denham, H.; Partridge, L. J.; Pluckthun, A.; Blackburn, G. M. *Angew. Chem., Int. Ed.* **2002**, *41*, 775.
113. Cesaro-Tadic, S.; Lagos, D.; Honegger, A.; Rickard, J. H.; Partridge, L. J.; Blackburn, G. M.; Pluckthun, A. *Nat. Biotechnol.* **2003**, *21*, 679.
114. Scanlon, T. S.; Prudent, J. R.; Schultz, P. G. *J. Am. Chem. Soc.* **1991**, *113*, 9397.
115. Gao, C. S.; Lavey, B. J.; Lo, C. H. L.; Datta, A.; Wentworth, P.; Janda, K. D. *J. Am. Chem. Soc.* **1998**, *120*, 2211.
116. Takahashi, N.; Kakinuma, K.; Shimazaki, K.; Takahashi, K.; Niihata, S.; Aoki, Y.; Matsushita, H.; Nishi, Y. *Eur. J. Biochem.* **1999**, *261*, 108.